



Frontiers

Water distribution across the mantle transition zone and its implications for global material circulation

Shun-ichiro Karato

Yale University, Department of Geology and Geophysics, New Haven, CT 06520, USA

ARTICLE INFO

Article history:

Accepted 23 November 2010

Available online 13 December 2010

Editor: R.W. Carlson

Keywords:

water
hydrogen
seismology
electrical conductivity
partial melting

ABSTRACT

Various methods for inferring the water distribution in Earth's mantle are reviewed including geochemical and geophysical methods. The geochemical approach using the water contents of basalts shows that the water content in the source regions of ocean island basalt is generally larger than that of the source region of mid-ocean ridge basalt, but the location of the source regions of ocean island basalts is poorly constrained. Geophysical approaches have potential of providing constraints on the spatial distribution of water but their usefulness depends critically on the sensitivity of geophysical observations to water content relative to other factors, in addition to the resolution of geophysical observations. Existing experimental data on the influence of water on seismologically observable properties and on electrical conductivity are reviewed. Frequently used seismological observations such as the anomalies in seismic wave velocities and of the topography on the mantle discontinuities are only weakly sensitive to water content but more sensitive to other factors such as the major element chemistry and temperature for a typical range of water contents. In contrast, electrical conductivity is highly sensitive to water content and only modestly sensitive to other factors such as temperature, oxygen fugacity and major element chemistry. Models of electrical conductivity–depth profiles are constructed where the influence of hydrogen and iron partitioning among coexisting minerals and of the depth variation in oxygen fugacity are incorporated. It is shown (i) that the electrical conductivity varies more than two orders of magnitude for a plausible range of water content in the mantle (~10 ppm wt to ~1 wt.%) and (ii) that if water content is constant with depth, there will be a drop in electrical conductivity at ~410-km. Although the resolution is not as high as seismological observations, geophysically inferred electrical conductivity distributions generally show higher conductivity in the mantle transition zone than the upper mantle, suggesting that the water content in the transition zone is higher than that in the upper mantle with some lateral variations. Implications of inferred water distribution are discussed including the possible partial melting near 410-km and its role in global water circulation.

© 2010 Elsevier B.V. All rights reserved.

1. Introduction

Water (hydrogen) is a unique component in terrestrial planets. Its abundance is small compared to other components (SiO_2 , MgO , CaO , etc.), yet even a small amount of water can modify the melting relationships (e.g., Inoue, 1994) and rheological properties (e.g., Karato and Jung, 2003; Mei and Kohlstedt, 2000) drastically. Consequently, the distribution of water has important influence on the dynamics and evolution of terrestrial planets.

In most of the previous studies on water in Earth's interior, focus has been placed on the solubility limit and/or the solubility mechanisms of water (hydrogen) in minerals particularly in nominally anhydrous minerals (e.g., Bolfan-Casanova, 2005; Inoue et al., 2010). Although there is still a major discrepancy about the water solubility in lower mantle minerals, it is clear that the total amount of

maximum water content in these minerals far exceeds the amount of ocean water. In particular, the observed high solubility of water in minerals in the mantle transition zone (the MTZ) suggests an important role of this layer in controlling the global water circulation. However, although these studies form an important basis for all studies on water in Earth, they are not sufficient to constrain the actual water distribution in Earth's interior. Actual water distribution in Earth's interior is only indirectly controlled by the solubility limit, and for example, even regions with high water solubility (e.g., the MTZ) could have little water (Richard et al., 2002).

Because diffusion is inefficient (diffusion distance is only ~10 km for one billion years calculated from the experimental results on chemical diffusion of water (Kohlstedt and Mackwell, 1998)), distribution of water in the real Earth is controlled largely by the location and degree of partial melting and by the large-scale material transport (e.g., Iwamori, 2007; Richard et al., 2006). However, in addition to partial melting that created the continental crust, the only well-recognized partial melting and resultant chemical segregation

E-mail address: shun-ichiro.karato@yale.edu.

are those associated with mid-ocean ridge volcanism (the former results in the long-term (2–3 Gyr or longer) geochemical signature, and the latter results in the relatively short-lived (less than 0.5 Gyr) geochemical signature). Neither the location nor the nature of large-scale mass transport in the deep mantle is well understood, and there have been widely different models for the water distribution in Earth's mantle (e.g., Hirschmann, 2006; Huang et al., 2005; Karato et al., 2006; Rüpke et al., 2006; Yoshino et al., 2008a). However, because there is a close link between water distribution and these processes, one can obtain new insights into the location of partial melting and the nature of materials circulation if the distribution of water is inferred as I will discussed later.

There have been many attempts to infer the water distribution in Earth's mantle (particularly the upper mantle and the MTZ). The most direct approach is the geochemical/geological approach in which one uses the water content of mantle minerals or the water content of basalt to infer the water distribution in Earth's mantle (e.g., Bell and Rossman, 1992; Beran and Libowitzky, 2006; Dixon et al., 2002). Although direct, this approach has a number of limitations, and in particular, this method provides only weak or no constraint on the distribution of water in critical regions such as the MTZ, one of the most important regions in terms of global water circulation.

Geophysical probes such as seismic waves and electromagnetic field penetrate deep into the Earth's mantle and the spatial distribution of relevant properties can be inferred from the surface observations. Consequently, geophysical observations provide data that could be used to infer water distribution in the deep mantle if their sensitivity to water content is high and well characterized (e.g., Karato, 2006b; Meier et al., 2009; Suetsugu et al., 2006). However, these studies showed widely different and sometimes puzzling conclusions. For example, using the anomalies in seismic wave velocity and in the topography on the seismic discontinuities, Meier et al. (2009) inferred the water-poor MTZ in the eastern Asia, whereas Suetsugu et al. (2006) inferred the water-rich MTZ in the same region. Similarly, there have been large discrepancies in the inferred water distribution from electrical conductivity (Huang et al., 2005; Yoshino et al., 2008a).

Therefore it seems important to examine the causes of the discrepancies in these studies, and to provide a better estimate of the water distribution in Earth's mantle. The purposes of this paper are (i) to review the various approaches for estimating the water distribution in Earth's mantle with particular emphasis on geophysical approaches, (ii) to provide a better estimate of water distribution in Earth's mantle and (iii) to discuss possible implications of the inferred water distribution for the nature of material circulation and partial melting in Earth. Issues on electrical conductivity have been discussed in some detail (Dai and Karato, 2009a; Karato and Dai, 2009) and consequently only a brief discussion on this topic will be presented, but important new results are added especially on the influence of element partitioning and of oxygen fugacity on electrical conductivity profiles.

2. Various approaches to infer the water distribution in the mantle

2.1. Geological/geochemical approach

Since the main focus in this paper is the evaluation and application of geophysical approach, only a brief summary of results from geochemical/geological approach is given here. For a more complete coverage, a reader is referred to some review papers on this topic and references therein (e.g., Beran and Libowitzky, 2006; Dixon et al., 2002).

The water contents of minerals in mantle rocks provide the most direct information on the water content of the mantle. The water contents in upper mantle samples range from ~0.002 to ~0.05 wt.%.

However, because diffusion of water is fast at the scale of xenoliths (~10 cm), it is not clear if the mantle rocks exposed at the Earth's surface preserve the water content when they were in the Earth's interior (e.g., Demouchy et al., 2006). In addition, one can study only limited regions by this method: the maximum depth from which mantle rocks are transported to the surface is ~200 km, so there is no constraint on water content of the MTZ from this approach.

In contrast, by using basalts, one can explore the water contents of broader regions because basaltic volcanism is the largest volcanism on Earth involving a large volume of the mantle. MORB (mid-ocean ridge basalt) is formed at the global scale by partial melting of the shallow mantle, and OIB (ocean island basalt) is formed by melting of materials coming from deeper regions or by melting of materials such as eclogite-rich rocks that contain a large amount of incompatible elements (Hofmann, 2004). Therefore this method provides constraints on the water distribution in the broad regions of the Earth's mantle. In this latter approach, one measures the water contents of basalts, and calculates the water contents of their source regions from which basalts are formed using a model of partial melting. The water content in the source region of MORB, i.e., the oceanic asthenosphere, is well constrained by this method (~0.01 wt.% with an error of a factor of ~2) (Dixon et al., 2002; Hirschmann, 2006). Most of OIB source regions have higher water contents (~0.075 wt.%) than the MORB source regions (Dixon et al., 2002). However, the interpretation of the data from OIB is not straightforward because the source regions of OIB are not well understood. In fact there are two classes of models for the OIB source regions: a layered mantle model (Albarède and van der Hilst, 2002; Allègre et al., 1996) and a plum pudding model (Davies, 1984; Rüpke et al., 2006; Sobolev et al., 2007). Distinguishing these models solely by geochemical approach is difficult.

2.2. Geophysical approach

In contrast to the geochemical approach, geophysical approaches provide wider sampling regions because geophysical probes (e.g., seismic or electromagnetic waves) penetrate to broader regions compared to geochemical sampling (Karato, 2006b). Consequently, one can place better constraints on the spatial distribution of water at a global scale by geophysical approaches. However, in using these approaches, it is critical to examine which properties are suitable for this purpose. Briefly, in order for a geophysical observable to be useful in inferring water content that observable must be sensitive to water content but insensitive to other variables or the correction for the influence of other variables must be made reliably.

2.2.1. Seismological observations

The most obvious effect of water on seismic wave propagation is the reduction of seismic wave velocities due to the weakened chemical bonding by hydrogen. Extensive experimental studies have been performed to investigate the influence of water content and other factors on elastic wave velocities using high-frequency techniques (Table 1: Jacobsen, 2006; Jacobsen and Smyth, 2006; Jacobsen et al., 2008; Mao et al., 2008). These studies show that the influence of water on high-frequency elastic wave velocities in mantle minerals is minor (<0.1%) for water content of less than ~0.1% when these effects are evaluated at relevant mantle conditions. These values are less than the influence of temperature (a temperature variation of 100 K will cause the velocity variation of ~0.7%, Karato, 2008a). In contrast, the influence of major element chemistry is large particularly in the MTZ. For example, pyrolyte and harzburgite composition will have a different amount of majorite and calcium-perovskite in the MTZ leading to variations in seismic wave velocities of a few % (Irfune et al., 2008; Nishiyama et al., 2009). I conclude that the influence of water on seismic wave velocity is small and less than that of plausible variations in the major element chemistry and in temperature (Fig. 1a). Therefore it is difficult to estimate water content where

Table 1

Water content dependence of seismic wave velocities. Parameters in the relation $V_{S/P}^{\infty}(T, C_W) = V_{S/P,0}^{\infty} \cdot (1 - \beta_{S/P,W}(C_W - C_{W0}))$ are given using the unit of wt.% for water content, C_W . $V_{S/P}^{\infty}$ is the S (P) wave velocity at the infinite frequency. The uncertainties in velocity measurements are typically 0.2–0.5% and the uncertainties in the estimated parameters of $\beta_{S/P,W}$ are typically $\pm 10\%$.

| | $\beta_{P,W}$ | $\beta_{S,W}$ | Reference |
|--------------------------|---------------|---------------|---------------------------|
| Olivine ^a | –0.0042 | –0.0052 | Jacobsen et al. (2008) |
| Wadsleyite ^b | –0.025 | –0.029 | Mao et al. (2008) |
| Ringwoodite ^c | –0.006 | –0.018 | Jacobsen and Smyth (2006) |

^a Results at room pressure and temperature.

^b Results at P = 12 GPa and room temperature.

^c Results at P = 20 GPa and room temperature. Calculated from Figure 7 of Jacobsen and Smyth (2006).

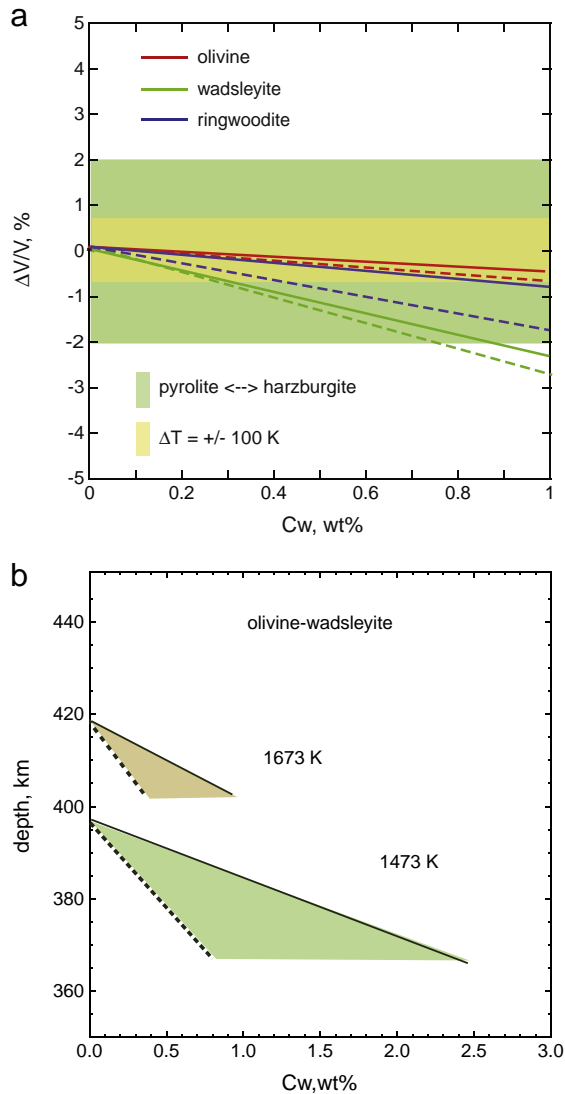


Fig. 1. Sensitivity of seismological observations to water content and other parameters. (a) Seismic wave velocities ($\Delta V/V$: variation of velocity, C_w : water content) (for data see Table 1). Solid lines are for P-wave velocities, and broken lines are for S-wave velocities. For olivine, results at room pressure and temperature are used. For wadsleyite, the results at 12 GPa, and for ringwoodite, results at ~ 20 GPa are used. (b) Depth of “410-km” discontinuity as a function of water content for two different temperatures (results for a pure $Mg_2SiO_4-H_2O$ system (Frost and Dolejš, 2007)). Above the solid lines only wadsleyite exists, and below the broken lines only olivine exists. Water affects the positions of these lines and hence both the depth of the “410-km” discontinuity and its sharpness (the distance between the solid and broken lines). A similar effect was observed for the “660-km” discontinuity.

variation in temperature and/or major element chemistry occurs. If the influence of anelasticity is included, the effect of water on seismic wave velocities will be larger (e.g., Karato, 2006b). For instance, if one uses the absorption band model, then the maximum amount of anelasticity is related to the magnitude of Q . For the PREM model (Dziewonski and Anderson, 1981), the influence of anelasticity on seismic wave velocities is up to $\sim 0.5\%$. However, the details of the influence of water on anelasticity are not known including the validity of the absorption band model.

Another potentially important seismological observation is the depth of seismic discontinuity. Most of the seismic discontinuities are caused by phase transformations. Wood (1995) suggested that the depths of phase boundaries may be affected by water if water partitions differently between two co-existing minerals. This phenomenon leads to two observable changes in the mantle discontinuity (Fig. 1b): a change in the sharpness of a phase transformation and a change in the depth (pressure) of a phase transformation. Both of these aspects have been studied experimentally (Chen et al., 2002; Frost and Dolejš, 2007; Litasov and Ohtani, 2007) and have been used to infer the water contents in the MTZ (Blum and Shen, 2004; Meier et al., 2009; Suetsugu et al., 2006; van der Meijde et al., 2003). In some studies, the anomalies in the width of the MTZ are used to infer the water content together with the anomalies in velocities (Meier et al., 2009). However, a recent experimental study showed that the contrast in water solubility between co-existing minerals such as olivine and wadsleyite becomes small at high temperatures and hence such effects are difficult to detect under most of the MTZ conditions (Frost and Dolejš, 2007). In contrast, other factors such as the influence of major element chemistry on seismic discontinuities are large and complex leading to the presence of multiple discontinuities (particularly near 660 km) (Deuss et al., 2006; Weidner and Wang, 2000). Therefore, again, I conclude that it is difficult to use these observations to infer the distribution of water. Meier et al. (2009) inferred puzzling water distribution from the anomalies in seismic wave velocities and the width of the MTZ: a water-poor MTZ in the western Pacific and below eastern Asia and a water-rich MTZ in the central Pacific. It is possible that such puzzling conclusions are caused by the insensitivity of these observations to water content. However, the problem of major element chemistry is less serious if regions of study have nearly homogeneous composition. The results of regional studies by Blum and Shen (2004), Coutier and Revenaugh (2006), and Suetsugu et al. (2006) showed conclusions similar to this study, and in these cases, seismological approach may also be useful.

Among the various seismological observations, seismic wave attenuation is likely sensitive to water content (Karato, 2003; Shito et al., 2006). However the resolution of attenuation measurements is limited (Dalton et al., 2009) and experimental studies are still exploratory (Aizawa et al., 2008). Further studies on the influence of water on seismic wave attenuation are needed to obtain better constraints on water distribution from seismological observations.

Some technical details on seismic wave velocities are given in Supplemental Material 1.

2.2.2. Electrical conductivity

2.2.2.1. General background. Although the resolution is less than some of the seismological observations, electrical conductivity of the Earth’s interior can be inferred from the analysis of electromagnetic induction (Rikitake, 1966). Because electrical conductivity is sensitive to water content as first suggested by Karato (1990), geophysically inferred electrical conductivity of Earth’s interior provides important constraints on the distribution of water (hydrogen). However, electrical conductivity of minerals is also controlled by the migration of other charged species, and therefore the relative contribution from different mechanisms must be evaluated carefully.

In most cases, electrical conductivity of a mineral is caused by the hopping of electrons between ferric and ferrous iron (also referred to as “polaron” conduction) or the migration of protons, and electrical conductivity can be expressed as

$$\sigma = A_1 \cdot f_{O_2}^{q_1}(P, T) \cdot \exp\left(-\frac{H_1^*}{RT}\right) + A_2 \cdot f_{O_2}^{q_2}(P, T) \cdot C_W^r \cdot \exp\left(-\frac{H_2^*(C_W)}{RT}\right) \quad (1)$$

where $A_{1,2}$ is the pre-exponential term, f_{O_2} is oxygen fugacity, $q_{1,2}$ is the oxygen fugacity exponent, C_W is the (total) water content, r is a constant that depends on the mechanism of electrical conduction, and $H_{1,2}^*$ is the activation enthalpy ($H_{1,2}^* = E_{1,2}^* + PV_{1,2}^*$, $E_{1,2}^*$: activation energy, $V_{1,2}^*$: activation volume). The first term corresponds to polaron conduction and the second term to proton conduction. The contribution from the diffusion of Mg (Fe) can also be included but the functional form for this mechanism is similar to polaron conduction and its influence is relatively small, less than a half order of magnitude at ~1600 K (Constable, 1993). The influence of major element chemistry is not explicitly shown in this formula, but the major element chemistry likely affects the pre-exponential factor and/or the activation energy. It was suggested that the activation energy for hydrogen conduction may depend on the water content (Yoshino et al., 2008a). However, the magnitude of this effect is small when the appropriate technique (the impedance spectroscopy) is used (Dai and Karato, 2009c; Yoshino et al., 2009). Some details of electrical conductivity are given in Supplemental Material 2.

In evaluating various published results on electrical conductivity measurements, some technical issues need to be examined. First, when electrical conduction in minerals is by the motion of ions (e.g., proton conduction), it is important to take data for a broad range of frequencies and make corrections for the polarization effects (impedance spectroscopy; Macdonald, 1987; Roberts and Tyburczy, 1991). The effect of polarization is large when the density of charge carrier is high, leading to a systematic bias in conductivity measurements. The use of low-frequency measurements leads to the underestimation of the contribution from proton conduction at high temperatures.

Second is the issue of water content measurements. It is difficult to prepare truly dry samples under high pressures, and samples prepared without adding water often contain a large amount of water (e.g., Nishihara et al., 2006; Yoshino et al., 2008a). I use the results from samples with less than a few ppm wt of water as the results for dry samples (for most of physical properties of mantle minerals, samples with less than ~10 ppm wt water show “dry” behavior, e.g., Dai and Karato, 2009c; Mei and Kohlstedt, 2000).

Third, and a related issue, is that the water content of a sample can change during an experiment. In order to make sure that the measured result corresponds to the reported water content, it is necessary to determine the water content of a sample both before and after each measurement, and make sure that the water content did not change much.

Table 2 provides a list of data sources on laboratory studies on electrical conductivity of upper mantle and MTZ minerals. Most of studies have shown that the dissolution of water enhances electrical conductivity. However, not all the published studies satisfy the criteria discussed above, and in these cases the interpretation of the data is difficult (see notes in Table 2). Therefore in the following discussions, I chose those results that satisfy all of the above criteria but I will also discuss results that do not satisfy them for comparison. Figure 2 shows the electrical conductivity of typical minerals (olivine, garnet and wadsleyite) as a function of water content for a range of plausible water content in Earth’s mantle (10^{-5} –1 wt.%) at a certain fixed pressure and temperature. This figure shows that the influence of water is large and the conductivity changes by a factor of 100 to 300 for this range of water content. Throughout this paper, I use the water

content determined by using the SIMS calibration (Aubaud et al., 2007; Bell et al., 2003).

Dependence of conductivity on other parameters (temperature, pressure, major element composition and oxygen fugacity) is reviewed in Supplemental Material 2. The major element chemistry such as Mg# ($100 \times Mg / (Mg + Fe)$) or the abundance of Ca and Al affects the conductivity by less than a factor of ~2. For a temperature variation of 100 K, conductivity will change by ~30% for proton conduction. The influence of variation in oxygen fugacity and major element chemistry is about a factor of 3 or less. Therefore I conclude that the influence of temperature, major element chemistry and other factors is much smaller than that of water (hydrogen) content.

What about the influence of partial melting? Shankland et al. (1981) concluded that in order to enhance conductivity by a factor of 10 by partial melting, one would need ~10% melt fraction but such a high melt fraction unlikely exists on Earth due to efficient compaction by gravity. Gaillard et al. (2008) proposed that the presence of a small amount of carbonatite melt might explain high conductivity. However, highly fortuitous conditions such as the presence of continuous carbonatite melt with high alkali content are needed in order to attribute the geophysically observed high conductivity to the presence of carbonate melt. For the asthenosphere, the observed electrical conductivity can be naturally explained by proton conduction in solid minerals assuming a petrologically inferred water content

Table 2

Data source for laboratory studies on electrical conductivity.

| Mineral | Source | Comments* | Method** |
|---------------|--------------------------|-----------|----------|
| Olivine | Wang et al. (2006) | x (1) | IS |
| | Yoshino et al. (2009) | x (2) | IS |
| | Yoshino et al. (2006) | (3) | LF |
| | Xu et al. (2000) | x (4) | IS |
| | Constable et al. (1992) | (5) | *** |
| | Poe et al. (2010) | (6) | IS |
| Orthopyroxene | Dai and Karato (2009a) | x (7) | IS |
| | Romano et al. (2006) | (8) | IS |
| | Yoshino et al. (2008b) | (9) | LF |
| Garnet | Dai and Karato (2009b) | x (10) | IS |
| | Huang et al. (2005) | (11) | IS |
| | Dai and Karato (2009c) | x (12) | IS |
| | Yoshino et al. (2008a) | (13) | LF |
| Wadsleyite | Manthilake et al. (2009) | (14) | LF |
| | Huang et al. (2005) | x (15) | IS |
| | Yoshino et al. (2008a) | (16) | LF |

*x: results used in the present calculation.

**IS: impedance spectroscopy.

***LF: low-frequency measurements.

***: Technique of conductivity measurements is not described in this paper, but since this study is on polaron (electronic) conduction, the technique used does not affect the results so much.

(1): Ni–NiO buffer. 4 GPa.

(2): Mo–MoO₂ buffer. 10 GPa.

(3): Ni–NiO buffer. 3 GPa.

(4): No measurements of water content. 4–10 GPa. Mo–MoO₂ buffer.

(5): fO₂ controlled by a CO–CO₂ mixture, close to Ni–NiO buffer. 0.1 MPa.

(6): Ni–NiO buffer. 8 GPa. Water content dependence of activation energy is reported. However, water content is reported only for samples after the measurements and therefore the possible role of changes in water content during measurements cannot be evaluated.

(7): Mo–MoO₂ buffer. 8 GPa. Only one sample for water-containing orthopyroxene (water content dependence of conductivity is assumed to be the same as olivine).

(8): Mo–MoO₂ buffer. 10–19 GPa. No measurements of water content.

(9): Majorite garnet. Mo–MoO₂ buffer. 18–23 GPa. Large uncertainties in water contents.

(10): Pyrope garnet. Mo–MoO₂ buffer. 4–16 GPa.

(11): Mo–MoO₂ buffer. ~14–15 GPa. Limited water content and temperature range.

(12): Mo–MoO₂ buffer. ~14–15 GPa.

(13): Mostly from low-frequency (0.1–0.01 Hz) measurements. A large amount of water in a “dry” sample.

(14): Essentially the same data as Yoshino et al. (2008a).

(15): Mo–MoO₂ buffer. ~15 GPa. Limited water content and temperature range.

(16): Mostly low-frequency (0.1–0.01 Hz) measurements. A large amount of water in a “dry” sample.

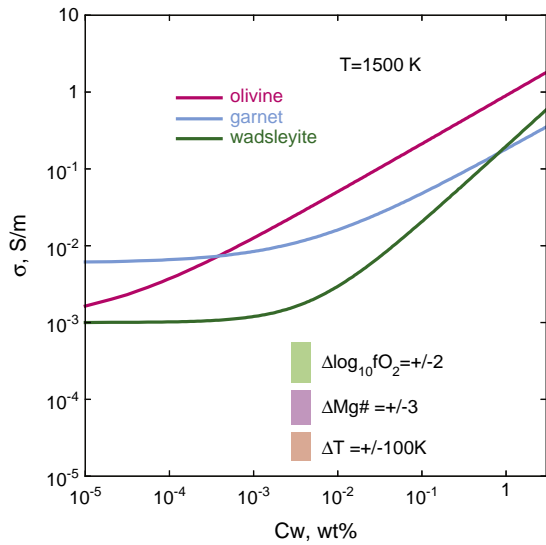


Fig. 2. Influence of water content (C_w) on electrical conductivity (σ) at 1500 K in olivine (4 GPa), garnet (4 GPa), and wadsleyite (15 GPa) at f_{O_2} (oxygen fugacity) corresponding to the Mo–MoO₂ buffer (data see Table 2). Shown together are the influence of other factors including the variation in temperature (T), Mg# and f_{O_2} (the height of each bar corresponds to the influence of each factor). The influence of mineralogy, such as pyrolite versus harzburgite can also be estimated from this figure.

(~0.01 wt.% with a factor of ~2 uncertainty; Dai and Karato, 2009a) and the presence of partial melt is not necessary to explain the high conductivity of the asthenosphere. Toffelmier and Tyburczy (2007) examined the possible influence of the presence of a thin partially molten layer atop the 410-km discontinuity. They concluded that such a layer is only marginally detectable by electromagnetic induction. I conclude that the influence of partial melting is minor compared to the influence of water.

2.2.2.2. Calculation of electrical conductivity–depth profiles for the model mantle. In order to obtain a better idea about how water content may influence the electrical conductivity, I have calculated the electrical conductivity versus depth profiles for various fixed water contents. In this calculation, a typical mantle geotherm was chosen (Ito and Katsura, 1989) (see Fig. 3a), and the influence of depth variation of oxygen fugacity and element partitioning is included.

The influence of oxygen fugacity is complicated because the pressure dependence of oxygen fugacity in laboratory experiments and in Earth's mantle is likely different. I used the depth-dependent oxygen fugacity model by Frost and McCammon (2008). The influence of pressure is, in general weak, but is included in these calculations. However, the influence of pressure on proton conduction was not studied in detail. The limiting data for pyrope (at 4 and 8 GPa) showed weak pressure sensitivity, but the discrepancy between the results for “wet” olivine by Wang et al. (2006) at 4 GPa and by Yoshino et al. (2009) at 10 GPa might be due to the influence of pressure. Consequently, I calculated the conductivity–depth profiles for both with and without pressure effects for “wet” olivine.

The most important parameter is the water content in each mineral that can change the conductivity up to three orders of magnitude. Consequently, for a given total water content, the water content in each mineral was calculated from the known solubility ratios (partition coefficients) of water (e.g., Bolfan-Casanova, 2005; Mookherjee and Karato, 2010). Iron content in each mineral is calculated using the reported partitioning of iron by Irifune and Isshiki (1998). Knowing the water and iron content in all co-existing minerals and the temperature and pressure, I calculated the electrical conductivity of each mineral and then calculated the electrical conductivity of an aggregate using the

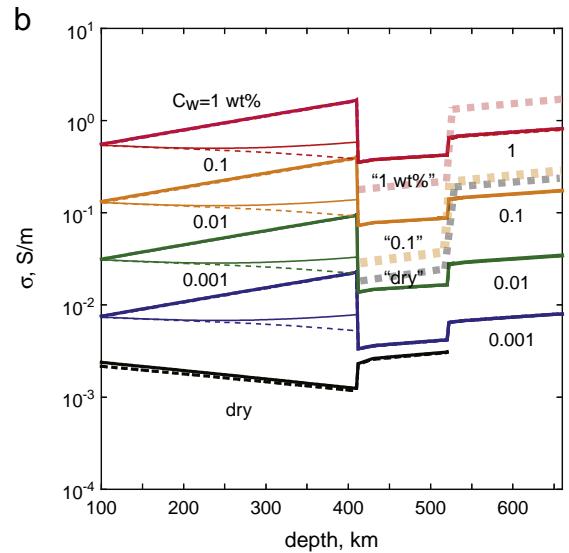
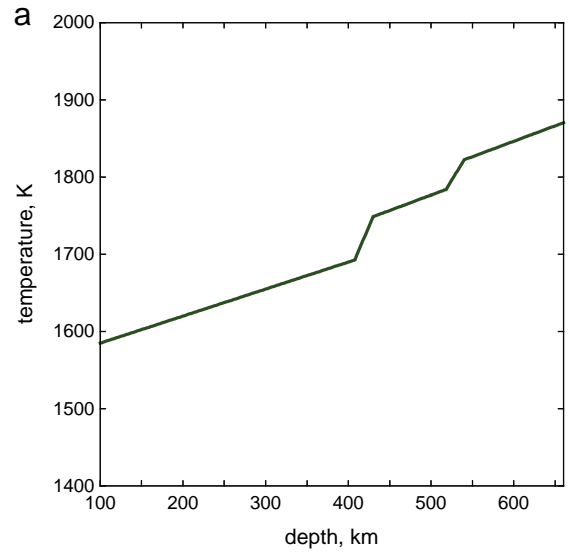


Fig. 3. (a) Temperature–depth profile used in the calculation of conductivity–depth profile (Ito and Katsura, 1989). (b) Electrical conductivity (σ) versus depth relationships for the upper mantle and the MTZ calculated for the pyrolite mantle model with various water contents. Solid lines correspond to the Hashin–Shtrikman upper bounds, and broken lines to the lower bound (differences are small in most cases). Thick lines are for models without pressure effects for “wet” olivine, thin lines are for the model with pressure effects. For comparison, results from Yoshino’s group for the MTZ are also shown by thick broken half-tone curves (Yoshino, 2010). These are based on low, one-frequency measurements and the “dry” samples in these studies contain substantial amounts of water (~0.01 wt.% or higher). No data for pyrope nor orthopyroxene was published from Yoshino’s group, and therefore results for the upper mantle from their lab are not shown. For the data source see Tables 2 and 3, and the details of method of calculation of conductivity–profiles are given in Supplemental Material 2.

Hashin and Shtrikman (1962) model (Supplemental Material 2). The parameter values for electrical conductivity of representative minerals under a standard condition are given in Table 3. Results of such calculations are shown in Figure 3b.

An important effect of water content on the electrical conductivity is clearly seen in Figure 3b, although the magnitude of water effect is smaller if the results by Yoshino (2010) that do not satisfy above criteria are used. The weaker effect of water by Yoshino (2010) is largely due to the higher values of “dry” conductivity due to the large water contents in their “dry” samples.

There is a drop in conductivity at 410-km from the upper mantle to the MTZ (its magnitude depends on the model for the pressure dependence). This is likely due to the differences in the nature of

Table 3
Parameters in electrical conductivity of typical mantle minerals at a reference condition (the reference condition for upper mantle minerals is the condition at 100-km depth, and that for transition zone minerals is either 410 km (wadsleyite and majorite garnet) or 520 km (ringwoodite)). The formula $\sigma = A \cdot \left(\frac{f_{O_2}}{f_{O_2,ref}}\right)^q \cdot C_W^r \cdot \exp\left(-\frac{E^* + PV^*}{RT}\right)$ is used where $f_{O_2,ref}$ is the oxygen fugacity at the reference state. When experimental data are for a certain oxygen fugacity buffer and Mg#, the results are normalized to the values of oxygen fugacity and Mg# at the reference depth. Conductivity of majorite garnet was not measured using the impedance spectroscopy under the well-controlled water content. However, based on a comparison of results by Romano et al. (2006) and Yoshino et al. (2008b), I assume that the electrical conductivity of garnet for a constant water content does not change markedly with the phase transformation. This causes some uncertainties in the transition zone conductivity, but the influence of this uncertainty is not large because electrical conductivity in the MTZ is controlled mostly by either wadsleyite or ringwoodite due to the higher hydrogen concentration in these minerals than in majorite garnet.

| | A (S/m) | q ^a | r | E* (kJ/mol) | V* (cc/mol) |
|---------------|-------------------|----------------|------|----------------|----------------|
| Olivine | 10 ^{2.4} | 0.17 | – | 154 | 2.4 |
| | 10 ^{3.1} | –0.1 | 0.62 | 87 | – ^b |
| Orthopyroxene | 10 ^{2.7} | 0.17 | – | 147 | – |
| | 10 ^{2.6} | –0.1 | 0.62 | 82 | – |
| Garnet | 10 ^{2.1} | 0.17 | – | 128 | 2.5 |
| | 10 ^{2.7} | –0.1 | 0.63 | 70 | –0.6 |
| Wadsleyite | 10 ^{2.1} | 0.17 | – | 147 | – |
| | 10 ^{2.1} | –0.1 | 0.72 | 88 | – |
| Ringwoodite | – | 0.17 | – | – | – |
| | 10 ^{3.6} | –0.1 | 0.69 | 104 | – |

The parameters for the top row are for polaron conduction and those for the bottom row are for proton conduction. The values of A are adjusted to an assumed value of parameters for a reference depth including the Mg# and oxygen fugacity.

Among the parameters, the most important are r and E* (and A) that represent water content dependence and temperature dependence. The uncertainties in these parameters are typically ± 5 –10 kJ/mol for E* (uncertainties of E* for electrical conductivity measurements are considerably smaller than those for creep or diffusion because of a larger number of data points and better reproducibility of measurements), ± 0.1 for r and for logA the uncertainties are ± 0.3 for proton conduction, and ± 0.1 for polaron conduction (this difference comes from the difference in the temperature range of measurements).

^a q is not well constrained except for the polaron conduction in olivine (Schock and Duba, 1985). For other materials, q is assumed to be 0.17 for polaron conduction, and also –0.10 for proton conduction (based on the results for wadsleyite (Dai and Karato, 2009c)). The influence of q on calculated conductivity profiles is relatively small (less than 50%) because the variation in oxygen fugacity is relatively small.

^b The effects of pressure on proton conduction are not well constrained. For olivine, the discrepancy in the existing data on hydrated samples implies that conductivity might be reduced by a factor of 10 from 4 GPa to 10 GPa (for explanations see text).

hydrogen-related defects between olivine and wadsleyite. According to the analysis by Karato (2006a), only a fraction of hydrogen (highly mobile hydrogen) dissolved in minerals contributes to electrical conductivity. The fraction of highly mobile hydrogen is smaller for wadsleyite than for olivine because of the deeper trapping of hydrogen in wadsleyite (wadsleyite has higher hydrogen solubility than olivine). Consequently, for the same total hydrogen content, electrical conductivity in wadsleyite is lower than that of olivine leading to a drop in conductivity at 410-km. Evidence of various hydrogen-related species was reported by Nishihara et al. (2008).

For comparison, I summarize the geophysically inferred electrical conductivity–depth profiles in Figure 4 (for the data source, see Table 4). A few general conclusions can be drawn from the comparison of these two figures. The truly “dry” model, i.e., polaron conduction model, predicts much lower conductivity than most of geophysical models. On average the water content in the upper mantle is on the order of ~0.01 wt.%, whereas it is ~0.1 wt.% for the MTZ. A model with a constant water content predicts a drop in conductivity at 410-km and is not consistent with most of geophysically inferred conductivity profiles. The above model is in excellent agreement with a geochemical/petrological model of the upper mantle (Dai and Karato, 2009a; Dixon et al., 2002; Hirschmann, 2006). Note, however, that the water content of the lower mantle is not constrained from electrical conductivity because there is no experimental data on the influence of water on the electrical conductivity of lower mantle minerals.

Electrical conductivity profiles also show large regional variations. For example, conductivity in the circum-Pacific (particularly east Asian) MTZ is high. Conductivity is low in the north-western part of the Pacific asthenosphere and in the central-south European MTZ (lower than that of the Pacific MTZ). The high water content in the east Asian MTZ is likely due to deep water transport by subduction of old plates and also models were proposed to explain low conductivity in the north-western Pacific upper mantle (Karato, 2008b) and in the central-south European MTZ (Maruyama and Okamoto, 2007).

In summary, electrical conductivity is sensitive to water content but insensitive to other parameters such as the major element

chemistry and oxygen fugacity (modestly sensitive to temperature). Consequently, electrical conductivity can be used to infer water distribution in Earth’s mantle. Results suggest both radially and laterally varying water content. In contrast, seismological observations can be used to infer water content only when the influence of other factors is well known. From the global inversion of surface wave data, Meier et al. (2009) inferred puzzling water distribution: water-poor MTZ in the western Pacific to eastern Asian regions and water-rich central Pacific MTZ, a trend that is opposite to the inference from electrical conductivity and from geological settings. It is likely that this puzzling conclusion is due to the high sensitivity of seismic signatures to factors other than water content when global data are used.

3. Implications for material circulation in Earth

The observed lateral and radial variation of electrical conductivity suggests large variations in water content (and in temperature), and, by inference, variations in other incompatible elements. The most efficient process to create variations in water content (and also other components) is partial melting and resultant melt–solid segregation, but other mechanisms of chemical segregation such as delamination of oceanic crust could also cause regional variations in water content.

Figure 5a shows a model of water distribution and material circulation consistent with electrical conductivity observations. There is a marked increase in water content across the 410-km discontinuity in this model suggesting partial melting at ~410-km and resultant melt–solid segregation (Bercovici and Karato, 2003; Karato et al., 2006). In this model, there is a major compositional stratification in the concentration of incompatible elements across the 410-km discontinuity, and the MTZ (and regions below) is likely to have a large amount of incompatible elements. In this model, the upper mantle is a residue of partial melting at ~410-km (Bercovici and Karato, 2003; Karato et al., 2006): the water content of the upper mantle (the asthenosphere) is controlled by the partial melting and melt segregation near the 410-km discontinuity in this model.

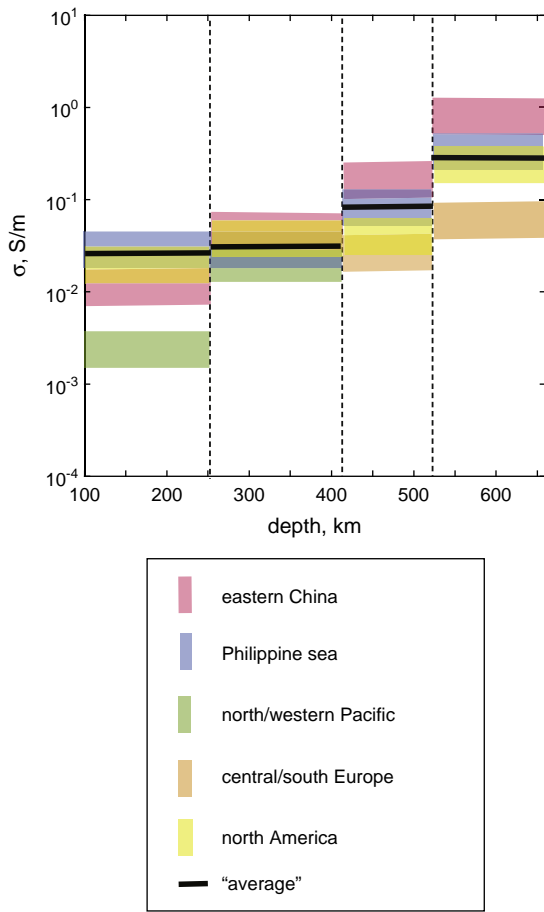


Fig. 4. Geophysically inferred conductivity (σ)–depth profiles. A piece-wise conductivity model is used. An “average” model shows a small increase in conductivity in the upper mantle followed by an increase in conductivity in MTZ. A constant water content model shown in Figure 3 is not consistent with this observation. In order to explain the increase in conductivity at 410-km discontinuity, an increase in water content at this depth is necessary. An “average model” can be attributed to ~ 0.01 wt.% water in the upper mantle and ~ 0.1 wt.% in the MTZ. However, a large lateral (regional) variation in conductivity is also observed suggesting a large regional variation in water content. For the data source see Table 4.

Figure 5b shows a model in which most of the mantle is depleted with water (and other incompatible components) with patchy distribution of water-rich regions in the lower mantle (Rüpke et al., 2006). The location of relatively water-rich regions (eclogite-rich regions) is not well constrained, but if these regions are considered to be distributed homogeneously or selectively in the lower mantle as presumed in some previous models (e.g., Albarède and van der Hilst,

2002; Rüpke et al., 2006; Tolstikhin and Hofmann, 2005), then this type of model is not consistent with the observed electrical conductivity profiles that show a marked increase in water at ~ 410 -km (compare Fig. 3b with Fig. 4).

Among the “plum-pudding model”, it is possible to make a model consistent with inferred layered water content (layered conductivity) if some modifications are made. Such a model is shown in Figure 5c where the fraction of relatively water-rich (eclogite) component is layered (the MTZ has a higher volume fraction of water-rich materials). OIB showing evidence of higher volume fraction of eclogite in their source regions (Sobolev et al., 2007) may come from eclogite-rich regions such as the MTZ (and/or deeper regions). If these relatively water-rich materials (eclogite) are connected or if these materials assume fine-scale layering in the MTZ, then the MTZ will have higher electrical conductivity than the upper mantle and such a model is consistent with the electrical conductivity observations. In order for this model to work, one needs (i) a mechanism to accumulate eclogite in the MTZ during subduction, say delamination of subducted oceanic crust in or near the MTZ (e.g., Karato, 1997) and (ii) to segregate eclogite component at the 410-km through upwelling say by selective partial melting of eclogite component at 410-km (due to the higher content of Fe, Ca, Al and H).

Models that are consistent with the inferred water distribution (either Fig. 5a or c) suggest partial melting at 410-km. Therefore it is worthwhile to revisit the global materials circulation model involving partial melting at 410-km (Bercovici and Karato, 2003; Karato et al., 2006). In this “water-filter” model, the asthenosphere is considered to be a residue of partial melting at 410-km. Hirschmann (2006) (see also Wood and Corgne, 2007) discussed that, assuming that the water content needed for partial melting at 410-km is ~ 0.4 wt.%, the water content of the upper mantle would be much larger than inferred from MORB chemistry (~ 0.01 wt.% with a factor of ~ 2 uncertainty), and hence this model is unlikely to be valid. However, this issue becomes less serious because the water content at the solidus is more likely ~ 0.05 wt.% as discussed by Karato et al. (2006) (see also a later paper by Hirschmann et al. (2009)).

Note also that if other volatile components such as carbon dioxide (Dasgupta and Hirschmann, 2006) or potassium (Wang and Takahashi, 2000) promote melting, then the solidus value of water content in minerals will be less than the values cited above. Furthermore, the actual water content of the upwelling residual materials that will become the asthenosphere (the source region for MORB) should be less than the water content in minerals at the solidus at 410-km. The water content of the asthenosphere in this model is approximately the water content at the solidus in the asthenosphere and not the water content at the solidus at ~ 410 -km if one assumes fractional melting (see Fig. 6) (there is a small amount of water in co-existing melt, but the volume fraction of co-existing melt is smaller than the degree of partial melting because of the high mobility of melt compared to the mobility of solid component) (see e.g., Spiegelman and Elliott (1993) and Spiegelman and Kenyon (1992)). The water content at the solidus in the asthenosphere is estimated to be ~ 0.01 wt.% (e.g., Hirschmann, 2010). Consequently, I conclude that the water content of the asthenosphere inferred from MORB composition and from electrical conductivity is compatible with the “water-filter” model.

What is the influence of partial melting (in the deep upper mantle) on geophysical signatures? The influence of partial melting on geophysical observables depends on the melt fraction, the contrast in physical properties between melt and solid, and the geometry of melt. If the melt fraction is $\sim 0.1\%$ as expected in the deep upper mantle, then partial melting does not have large effects (less than $\sim 1\%$ reduction) on seismic wave velocities if melt occurs as tubules (e.g., Shankland et al., 1981; Takei, 2002), whereas if melt completely wets grain-boundaries, then the velocity reduction can be much higher ($\sim 10\%$, e.g., Zener, 1941). Consequently, low velocity regions are expected below the critical depth below which complete wetting occurs (d_{wet}) and 410-km.

Table 4

Data for geophysically inferred electrical conductivity distribution.

| Region | Reference | Comments |
|-----------------------|---|----------|
| Global | Kelbert et al. (2009) | (1) |
| Eastern Asia | Ichiki et al. (2006) | |
| Philippine sea | Ichiki et al. (2001), Seama et al. (2007), and Shimizu et al. (2010a,b) | |
| Central/north Pacific | Kuvshinov and Olsen (2006), Shimizu et al. (2010a,b), and Utada et al. (2003) | |
| Central-south Europe | Tarits et al. (2004) and Utada et al. (2009) | |
| North America | Neal et al. (2000) | (2) |

(1) Poor resolution for the shallow upper mantle because of the use of relatively low frequency data. This paper contains a summary of other papers on various regions.

(2) There are large variations in the conductivity in the North America. The values shown in Figure 5 are from Neal et al. (2000), but the results from the Canadian Shield gives a lower conductivity in the upper mantle (Schultz et al., 1993).

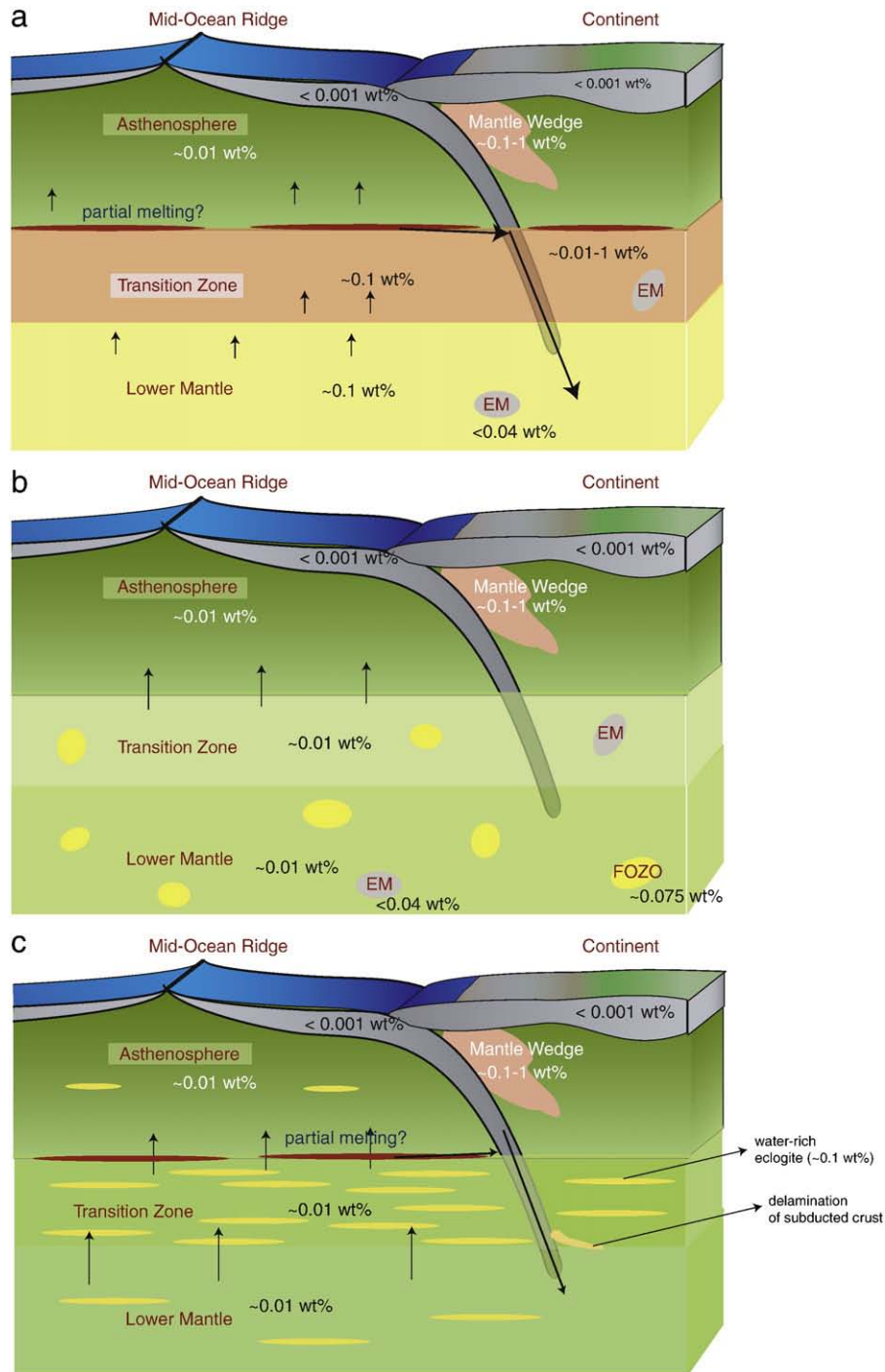


Fig. 5. Models of water distribution and material circulation in Earth's mantle. (a) A layered water content model based on the combination of geochemical observations on water in basalts and geophysical observations of electrical conductivity interpreted by mineral physics data. Water content in the mantle is layered (with some lateral variations). A broad region of the deep mantle, below the MTZ is relatively water-rich (~ 0.1 wt.%) that is a source region of OIB, and a relatively water-poor region in the upper mantle (asthenosphere) is the source region of MORB. This model suggests partial melting at 410-km discontinuity but not at 660-km discontinuity. (b) A "plum-pudding" model of water distribution model proposed by Rüpke et al. (2006) based on the geochemical observations of water in basalts and a single-stage model of water circulation assuming that water-rich regions are in the lower mantle. In this model the source regions of OIB occur as patchy regions occupying $\sim 7\%$ of the mantle. If water-rich regions occur homogeneously or only in the lower mantle, then such a model is not supported by the observation of electrical conductivity. (c) A hybrid "plum-pudding" model of water distribution involving two components. In this model, the volume fraction of water-rich (eclogitic material) is considered to be higher in the MTZ than the upper mantle. MORB is formed by partial melting of relatively eclogite-poor materials, and OIB is formed by partial melting of eclogite-rich materials. If eclogitic materials are connected or if they are distributed as fine lamellae, then the MTZ will have higher conductivity than the upper mantle being consistent with the electrical conductivity observations. The lower mantle may have a similar amount of eclogite but there is no constraint on the water content in the lower mantle.

Globally distributed low velocity regions in the deep upper mantle reported by Tauzin et al. (2010) may correspond to such regions, providing evidence for the large-scale occurrence of partial melting at

around 410-km. The influence of partial melting on electrical conductivity is, however, minor (less than a factor of ~ 2) even if melt completely wets grain-boundaries if melt fraction is less than $\sim 0.1\%$

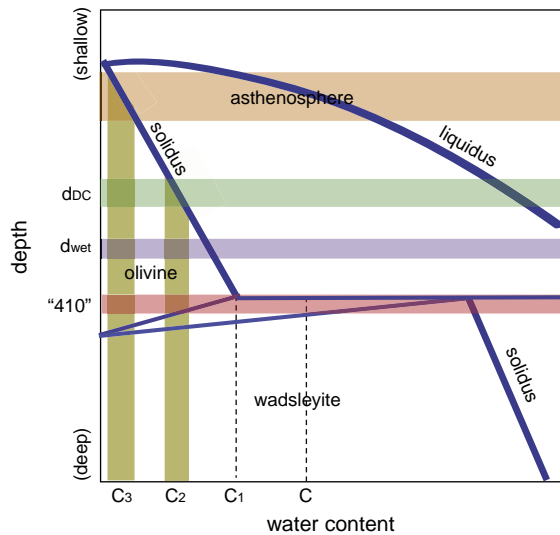


Fig. 6. A schematic phase diagram showing the melting behavior of a material containing water as impurity in the upper mantle and the shallow transition zone (adiabatic temperature gradient is assumed). Finite solubility of water in the solid component is assumed. When a material moves upwards, melting will occur at (or near) 410-km if the initial water content, C , exceeds C_1 . Upon melting, residual solids have the water content of C_1 and melt quickly sinks to the 410-km discontinuity (I assume heavy melt here). As a material moves upwards, partial melting continues, and if partial melting occurs as fractional melting, then the water content in the residual materials follows that at the solidus. Consequently, the water content in the asthenosphere in this model is the water content at the solidus under the asthenosphere pressures (C_3). Two depths are also important in understanding the global material circulation and the consequence of partial melting on physical properties. One is d_{DC} (water content at this depth is C_2), the depth below which the melt density is larger than the density of co-existing minerals. Below this level, melts will sink to the 410-km discontinuity, whereas above this depth, melt will rise to the bottom of the lithosphere. Also, there is a critical depth, d_{wet} , below which melt wets grain-boundaries but above which melt occurs as tubules (Yoshino et al., 2007). Seismic velocities are significantly reduced between d_{wet} and 410-km (but not above d_{wet}), whereas the influence of partial melting on electrical conductivity is always small. C_1 is estimated to be ~ 0.05 wt.% (Hirschmann et al., 2009; Karato et al., 2006) if water is the only volatile (incompatible) component and C_3 is estimated to be ~ 0.01 wt.% (e.g., Hirschmann, 2010).

(e.g., McLachlan et al., 1990; Shankland et al., 1981). Therefore partial melting in the deep upper mantle (or in the MTZ) will only have a modest effect in the interpretation of conductivity profiles.

Currently, we have no mineral physics data to infer the water content of the lower mantle. Therefore current electrical conductivity observations do not rule out a model of the lower mantle water content similar to that of the upper mantle (Hirschmann, 2006; Rüpke et al., 2006). Given an inferred high water content in the MTZ, such a model would imply partial melting at the 660-km discontinuity. However, no strong evidence has been reported for partial melting near that boundary. There is an urgent need for determining the water content dependence of electrical conductivity of the lower mantle minerals to address this issue from the geophysical observations. Also, high-resolution seismological observations such as receiver-function studies to detect possible partially molten layer near the 660-km discontinuity will be useful to test this model. Similarly, my analysis does not rule out deep hidden reservoirs of incompatible elements in the deep mantle such as the D'' layer. It is possible that both the MTZ and deep hidden reservoirs act as source regions of OIB.

Finally, let me discuss some possible implications of inferred water distribution on the evolution of the ocean mass. Solid Earth and ocean (+ crust) interactions occur through material circulation associated with plate tectonics. Volcanism such as the mid-ocean ridge volcanism brings water to the surface by *degassing*. In contrast, at subduction zones, water goes back to the mantle carried by sediments, hydrated crust and/or upper mantle. Water carried by subducting lithosphere will go back to the mantle (*regassing*). The ocean mass (and the water mass in the mantle) is controlled by the

dynamic balance of these processes (Franck and Bounama, 2001; McGovern and Schubert, 1989; Rüpke et al., 2006). In all previous models of global water circulation, the mantle was treated as a single unit that corresponds to the assumption of no deep mantle chemical segregation. In these models, the ocean mass at the dynamic equilibrium is directly proportional to degassing/regassing rate ratio and the ocean mass is highly sensitive to degassing/regassing rates (Supplemental Material 3, see also Franck and Bounama (2001)), and, by assumption, mantle has uniform water content. The present analysis shows that such models are not consistent with the observed electrical conductivity profiles and suggests deep mantle (~ 410 -km) melting or some chemical segregation. If such deep mantle segregation including partial melting occurs, then the mantle needs to be treated as a box with an internal variable (or two or more boxes). This will modify the sensitivity of the ocean mass to degassing/regassing parameters and might influence the stability of the ocean mass. A simple model is discussed in Supplemental Material 3, where the sensitivity of ocean mass to the degassing/regassing parameters is analyzed for the case of dynamic equilibrium. It is shown that melting in the MTZ buffers the ocean mass if the rate of water transport from the deep mantle to the upper mantle is fast compared to the rate of water transport from the deep mantle to the oceans.

4. Summary and concluding remarks

Distribution of water in Earth's mantle can be inferred by a combination of approaches. Geological/geochemical observations provide a robust estimate of water content for source regions of basalts, but the spatial distribution of water is poorly constrained particularly for the source region of OIB. Spatial distribution of water content can be better inferred by geophysical approaches. Among various geophysical observables, electrical conductivity is the most useful property to infer water content because it is highly sensitive to water content and only modestly influenced by other factors. In contrast, most of the seismological observations are sensitive to other factors such as major element chemistry and sensitivity to water content is small under most of the deep mantle conditions.

The major challenge, however, is the relatively poor resolution of geophysical inference of electrical conductivity. Recent studies show that better models of conductivity profiles can be obtained through the use of ocean bottom electromagnetometers (Seama et al., 2007). Also by using a global data set with improved inversion schemes, a three-dimensional distribution of electrical conductivity is becoming available down to the shallow lower mantle (Kelbert et al., 2009). In order to improve the resolution of inference of water distribution, it is critical to have better coverage of stations for these observations.

Equally critical is the improved knowledge on the water solubility and the role of water on electrical conductivity and other physical properties in lower mantle minerals. Currently, any models of global water circulation suffer from the lack of constraints on water distribution for the lower mantle. A combination of improved geophysical observations on electrical conductivity with the improved mineral physics studies on the role of water in lower mantle minerals will help us understand the evolution of this planet including the link between the solid Earth and the hydrosphere.

Acknowledgments

This study is supported by the National Science Foundation. Most of the electrical conductivity measurements were conducted by my colleagues including Yousheng Xu, Xiaoge Huang, Doujung Wang, Mainak Mookherjee and Lidong Dai. I thank the following people for various discussions: Adam Schultz, Anna Kelbert and Gary Egbert, and Kiyoshi Baba for geophysical studies on electrical conductivity, Toru Inoue for water solubility, Dan Frost for oxygen fugacity, Nori Nishiyama for elasticity, Arwen Deuss, Lev Vinnik and Eric Debayle for

seismological observations, and Dave Bercovici for the mechanisms of water transport. Rick Carlson made helpful editorial suggestions to improve the presentation of this paper.

Appendix A. Supplementary data

Supplementary data to this article can be found online at doi:10.1016/j.epsl.2010.11.038.

References

- Aizawa, Y., et al., 2008. Seismic properties of Anita Bay dunite: an exploratory study of the influence of water. *J. Petrol.* 49, 841–855.
- Albarède, F., van der Hilst, R.D., 2002. Zoned mantle convection. *Philos. Trans. R. Soc. Lond.* A360, 2569–2592.
- Allègre, C.J., Hofmann, A.W., O'Nions, K., 1996. The argon constraints on mantle structure. *Geophys. Res. Lett.* 23, 3555–3557.
- Aubaud, C., et al., 2007. Intercalibration of FTIR and SIMS for hydrogen measurements in glasses and nominally anhydrous minerals. *Am. Mineralog.* 92, 811–828.
- Bell, D.R., Rossman, G.R., 1992. Water in Earth's mantle: the role of nominally anhydrous minerals. *Science* 255, 1391–1397.
- Bell, D.R., Rossman, G.R., Maldener, J., Endisch, D., Rauch, F., 2003. Hydroxide in olivine: a quantitative determination of the absolute amount and calibration of the IR spectrum. *J. Geophys. Res.* 108. doi:10.1029/2001JB000679.
- Beran, A., Libowitzky, E., 2006. Water in natural mantle minerals II: olivine, garnet and accessory minerals. In: Keppler, H., Smyth, J.R. (Eds.), *Water in Nominally Anhydrous Minerals*. Mineralogical Society of America, Washington DC, pp. 169–191.
- Bercovici, D., Karato, S., 2003. Whole mantle convection and transition-zone water filter. *Nature* 425, 39–44.
- Blum, J., Shen, Y., 2004. Thermal, hydrous, and mechanical states of the mantle transition zone beneath southern Africa. *Earth Planet. Sci. Lett.* 217, 367–378.
- Bolfan-Casanova, N., 2005. Water in the Earth's mantle. *Mineralog. Mag.* 69, 229–257.
- Chen, J., Inoue, T., Yurimoto, H., Weidner, D.J., 2002. Effect of water on olivine-wadsleyite phase boundary in the (Mg,Fe)₂SiO₄ system. *Geophys. Res. Lett.* 29. doi:10.1029/2001GR1014429.
- Constable, S., 1993. Constraints on mantle electrical conductivity from field and laboratory measurements. *J. Geomagnetism Geoelectricty* 45, 707–728.
- Constable, S., Shankland, T.G., Duba, A., 1992. The electrical conductivity of an isotropic olivine mantle. *J. Geophys. Res.* 97, 3397–3404.
- Coutier, A.M., Revenaugh, J., 2006. A water-rich transition zone beneath the eastern United States and Gulf of Mexico from multiple ScS reverberations. In: Jacobsen, S.D., van der Lee, S. (Eds.), *Earth's Deep Water Cycle*. American Geophysical Union, Washington DC, pp. 181–193.
- Dai, L., Karato, S., 2009a. Electrical conductivity of orthopyroxene: implications for the water content of the asthenosphere. *Proc. Jpn Acad.* 85, 466–475.
- Dai, L., Karato, S., 2009b. Electrical conductivity of pyrope-rich garnet at high temperature and pressure. *Phys. Earth Planet. Inter.* 176, 83–88.
- Dai, L., Karato, S., 2009c. Electrical conductivity of wadsleyite under high pressures and temperatures. *Earth Planet. Sci. Lett.* 287, 277–283.
- Dalton, C.A., Ekström, G., Dziewonski, A.M., 2009. Global seismological shear velocity and attenuation: a comparison with experimental observations. *Earth Planet. Sci. Lett.* 284, 65–75.
- Dasgupta, R., Hirschmann, M.M., 2006. Melting in the Earth's deep mantle caused by carbon dioxide. *Nature* 440, 659–662.
- Davies, G.F., 1984. Geophysical and isotopic constraints on mantle convection: an interim synthesis. *J. Geophys. Res.* 89, 6017–6040.
- Demouchy, S., Jacobsen, S.D., Gaillard, F., Stern, C.R., 2006. Rapid magma ascent recorded by water diffusion profiles in mantle olivine. *Geology* 34, 429–432.
- Deuss, A., Redfern, S.A.T., Chambers, K., Woodhouse, J.H., 2006. The nature of the 660-kilometer discontinuity in Earth's mantle from global seismic observations of PP precursors. *Science* 311, 198–201.
- Dixon, J.E., Leist, L., Langmuir, J., Schilling, J.G., 2002. Recycled dehydrated lithosphere observed in plume-influenced mid-ocean-ridge basalt. *Nature* 420, 385–389.
- Dziewonski, A.M., Anderson, D.L., 1981. Preliminary reference Earth model. *Phys. Earth Planet. Inter.* 25, 297–356.
- Franck, S., Bounama, C., 2001. Global water cycle and Earth's thermal evolution. *J. Geodyn.* 32, 231–246.
- Frost, D.J., Dolejš, D., 2007. Experimental determination of the effect of H₂O on the 410-km seismic discontinuity. *Earth Planet. Sci. Lett.* 256, 182–195.
- Frost, D.J., McCammon, C., 2008. The redox state of Earth's mantle. *Annu. Rev. Earth Planet. Sci.* 36, 389–420.
- Gaillard, F., Malki, M., Iacono-Maziano, G., Pichavant, M., Scailliet, B., 2008. Small amount of carbonate melts explains high electrical conductivity in the asthenosphere. *Science* 322, 1363–1365.
- Hashin, Z., Shtrikman, S., 1962. A variational approach to the theory of effective magnetic permeability of multiphase materials. *J. Appl. Phys.* 33, 3125–3131.
- Hirschmann, M.M., 2006. Water, melting, and the deep Earth H₂O cycle. *Annu. Rev. Earth Planet. Sci.* 34, 629–653.
- Hirschmann, M.M., 2010. Partial melt in the oceanic low velocity zone. *Phys. Earth Planet. Inter.* 179, 60–71.
- Hirschmann, M.M., Tenner, T., Aubaud, C., Withers, A.C., 2009. Dehydration melting of nominally anhydrous mantle: the primacy of partitioning. *Phys. Earth Planet. Inter.* 176, 54–68.
- Hofmann, A.W., 2004. Sampling mantle heterogeneity through oceanic basalts: isotopes and trace elements. In: Holland, H.D., Turekian, K.K. (Eds.), *Treatise on Geochemistry*. Elsevier, Amsterdam, pp. 61–101.
- Huang, X., Xu, Y., Karato, S., 2005. Water content of the mantle transition zone from the electrical conductivity of wadsleyite and ringwoodite. *Nature* 434, 746–749.
- Ichiki, M., Baba, K., Obayashi, M., Utada, H., 2006. Water content and geotherm in the upper mantle above the stagnant slab: interpretation of electrical conductivity and seismic P-wave velocity models. *Phys. Earth Planet. Inter.* 155, 1–15.
- Ichiki, M., et al., 2001. Upper mantle conductivity structure of the back-arc region beneath northeastern China. *Geophys. Res. Lett.* 28, 3773–3776.
- Inoue, T., 1994. Effect of water on melting phase relations and melt composition in the system Mg₂SiO₄–MgSiO₃–H₂O up to 15 GPa. *Phys. Earth Planet. Inter.* 85, 237–263.
- Inoue, T., Wada, T., Sasaki, R., Yurimoto, H., 2010. Water partitioning in the Earth's mantle. *Phys. Earth Planet. Inter.* 183, 245–251.
- Irfune, T., Higo, Y., Inoue, T., Ohfuji, H., Funakoshi, K., 2008. Sound velocities of majorite garnet and the composition of the mantle transition zone. *Nature* 451, 814–817.
- Irfune, T., Isshiki, M., 1998. Iron partitioning in a pyrolite mantle and the nature of the 410-km seismic discontinuity. *Nature* 392, 702–705.
- Ito, E., Katsura, T., 1989. A temperature profile of the mantle transition zone. *Geophys. Res. Lett.* 16, 425–428.
- Iwamori, H., 2007. Transportation of H₂O beneath the Japan arcs and its implications for global water circulation. *Chem. Geol.* 239, 182–198.
- Jacobsen, S.D., 2006. Effect of water on the equation of state of nominally anhydrous minerals. In: Keppler, H., Smyth, J.R. (Eds.), *Water in Nominally Anhydrous Minerals*. Mineralogical Society of America, Washington DC, pp. 321–342.
- Jacobsen, S.D., et al., 2008. Effects of hydration on the elastic properties of olivine. *Geophys. Res. Lett.* 35. doi:10.1029/2008GL034398.
- Jacobsen, S.D., Smyth, J.R., 2006. Effect of water on the sound velocities of ringwoodite in the transition zone. In: Jacobsen, S.D., Lee, S.v.d. (Eds.), *Earth's Deep Water Cycle*. American Geophysical Union, Washington DC, pp. 131–145.
- Karato, S., 1990. The role of hydrogen in the electrical conductivity of the upper mantle. *Nature* 347, 272–273.
- Karato, S., 1997. On the separation of crustal component from subducted oceanic lithosphere near the 660 km discontinuity. *Phys. Earth Planet. Inter.* 99, 103–111.
- Karato, S., 2003. Mapping water content in Earth's upper mantle. In: Eiler, J.E. (Ed.), *Inside the Subduction Factory*. American Geophysical Union, Washington DC, pp. 135–152.
- Karato, S., 2006a. Influence of hydrogen-related defects on the electrical conductivity and plastic deformation of mantle minerals: a critical review. In: Jacobsen, S.D., van der Lee, S. (Eds.), *Earth's Deep Water Cycle*. American Geophysical Union, Washington DC, pp. 113–129.
- Karato, S., 2006b. Remote sensing of hydrogen in Earth's mantle. In: Keppler, H., Smyth, J.R. (Eds.), *Water in Nominally Anhydrous Minerals*. Mineralogical Society of America, Washington DC, pp. 343–375.
- Karato, S., 2008a. *Deformation of Earth Materials: Introduction to the Rheology of the Solid Earth*. Cambridge University Press, Cambridge, 463 pp.
- Karato, S., 2008b. Insights into the nature of plume–asthenosphere interaction from central Pacific geophysical anomalies. *Earth Planet. Sci. Lett.* 274, 234–240.
- Karato, S., Bercovici, D., Leahy, G., Richard, G., Jing, Z., 2006. Transition zone water filter model for global material circulation: where do we stand? In: Jacobsen, S.D., van der Lee, S. (Eds.), *Earth's Deep Water Cycle*. American Geophysical Union, Washington DC, pp. 289–313.
- Karato, S., Dai, L., 2009. Comments on “Electrical conductivity of wadsleyite as a function of temperature and water content” by Manthilake et al. *Phys. Earth Planet. Inter.* 174, 19–21.
- Karato, S., Jung, H., 2003. Effects of pressure on high-temperature dislocation creep in olivine polycrystals. *Philos. Mag.* A 83, 401–414.
- Kelbert, A., Schultz, A., Egbert, G., 2009. Global electromagnetic induction constraints on transition-zone water content variations. *Nature* 460, 1003–1006.
- Kohlstedt, D.L., Mackwell, S.J., 1998. Diffusion of hydrogen and intrinsic point defects in olivine. *Z. Physikische Chem.* 207, 147–162.
- Kuvshinov, A., Olsen, N., 2006. A global model of mantle conductivity derived from 5 years of CHAMP, Ørsted, and SAC-C magnetic data. *Geophys. Res. Lett.* 33. doi:10.1029/2006GL027083.
- Litasov, K.D., Ohtani, E., 2007. Effect of water on the phase relations in Earth's mantle and deep water cycle. In: Ohtani, E. (Ed.), *Advances in High-Pressure Mineralogy*. Geological Society of America, pp. 115–156.
- Macdonald, J.R. (Ed.), 1987. *Impedance Spectroscopy*. John Wiley & Sons, New York, 346 pp.
- Manthilake, M.A.G.M., et al., 2009. Electrical conductivity of wadsleyite as a function of temperature and water content. *Phys. Earth Planet. Inter.* 174, 10–18.
- Mao, Z., et al., 2008. Elasticity of hydrous wadsleyite to 12 GPa: implications for Earth's transition zone. *Geophysical Research Letters* 35. doi:10.1029/2008GL035618.
- Maruyama, S., Okamoto, K., 2007. Water transportation from the subducting slab into the mantle transition zone. *Gondwana Res.* 11, 148–165.
- McGovern, P.J., Schubert, G., 1989. Thermal evolution of the Earth: effects of volatile exchange between atmosphere and interior. *Earth Planet. Sci. Lett.* 96, 27–37.
- McLachlan, D.S., Blazkiewicz, M., Newham, R.E., 1990. Electrical resistivity of composite. *J. Am. Ceram. Soc.* 73, 2187–2203.
- Mei, S., Kohlstedt, D.L., 2000. Influence of water on plastic deformation of olivine aggregates. 2. Dislocation creep regime. *J. Geophys. Res.* 105, 21471–21481.
- Meier, U., Trampert, J., Curtis, A., 2009. Global variations of temperature and water content in the mantle transition zone from higher mode surface waves. *Earth Planet. Sci. Lett.* 282, 91–101.

- Mookherjee, M., Karato, S., 2010. Solubility of water in pyrope-rich garnet at high pressure and temperature. *Geophys. Res. Lett.* 37. doi:10.1029/2009GL041289.
- Neal, S.L., Mackie, R.L., Larsen, J.C., Schultz, A., 2000. Variations in the electrical conductivity of the upper mantle beneath North America and the Pacific ocean. *J. Geophys. Res.* 105, 8229–8242.
- Nishihara, Y., Shinmei, T., Karato, S., 2006. Grain-growth kinetics in wadsleyite: effects of chemical environment. *Phys. Earth Planet. Inter.* 154, 30–43.
- Nishihara, Y., Shinmei, T., Karato, S., 2008. Effects of chemical environments on the hydrogen-defects in wadsleyite. *Am. Mineralog.* 93, 831–843.
- Nishiyama, N., Kato, T., Irifune, T., Wada, K., 2009. Phase relations in harzburgite: Stagnation of harzburgite at the lower part of the mantle transition zone and interpretation of seismic discontinuity at 600 km depth. *EOS 90*, D11A-07.
- Poe, B., Romano, C., Nestola, F., Smyth, J.R., 2010. Electrical conductivity anisotropy of dry and hydrous olivine at 8 GPa. *Phys. Earth Planet. Inter.* 181, 103–111.
- Richard, G., Bercovici, D., Karato, S., 2006. Slab dehydration in the Earth's mantle transition zone. *Earth Planet. Sci. Lett.* 251, 156–167.
- Richard, G., Monnereau, M., Ingrin, J., 2002. Is the transition zone an empty water reservoir? Inference from numerical model of mantle dynamics. *Earth Planet. Sci. Lett.* 205, 37–51.
- Rikitake, T., 1966. *Electromagnetism and the Earth's Interior*. Elsevier, Amsterdam. 308 pp.
- Roberts, J., Tyburczy, J.A., 1991. Frequency dependent electrical properties of polycrystalline olivine compacts. *J. Geophys. Res.* 96, 16205–16222.
- Romano, C., Poe, B.T., Kredie, N., McCammon, C., 2006. Electrical conductivity of pyrope-almandine garnets up to 19 GPa and 1700 °C. *Am. Mineralog.* 91, 1371–1377.
- Rüpke, L.H., Phipps Morgan, J., Dixon, J.E., 2006. Implications of subduction rehydration for Earth's deep water cycle. In: Jacobsen, S.D., Lee, S.v.d. (Eds.), *Earth's Deep Water Cycle*. American Geophysical Union, Washington DC, pp. 263–276.
- Schock, R.N., Duba, A., 1985. Point defects and the mechanisms of electrical conduction in olivine. In: Schock, R.N. (Ed.), *Point Defects in Minerals*. American Geophysical Union, Washington DC, pp. 88–96.
- Schultz, A., Kurz, R.D., Chave, A.D., Jones, A.G., 1993. Conductivity discontinuities in the upper mantle beneath a stable craton. *Geophys. Res. Lett.* 20, 2941–2944.
- Seama, N., et al., 2007. 1-D electrical conductivity structure beneath the Philippine Sea: results from an ocean bottom magnetotelluric survey. *Phys. Earth Planet. Inter.* 162, 2–12.
- Shankland, T.J., O'Connell, R.J., Waff, H.S., 1981. Geophysical constraints on partial melt in the upper mantle. *Rev. Geophys. Space Phys.* 19, 394–406.
- Shimizu, H., Koyama, T., Baba, K., Utada, H., 2010a. Revised 1-D mantle electrical conductivity structure beneath the north Pacific. *Geophys. J. Int.* 180, 1030–1048.
- Shimizu, H., Utada, H., Baba, K., Koyama, T., Obayashi, M., Fukao, Y., 2010b. Three-dimensional imaging of electrical conductivity in the mantle transition zone beneath the North Pacific Ocean by a semi-global induction study. *Phys. Earth Planet. Inter.* 183, 252–269.
- Shito, A., Karato, S., Matsukage, K.N., Nishihara, Y., 2006. Toward mapping water content, temperature and major element chemistry in Earth's upper mantle from seismic tomography. In: Jacobsen, S.D., Lee, S.v.d. (Eds.), *Earth's Deep Water Cycle*. American Geophysical Union, Washington DC, pp. 225–236.
- Sobolev, A.V., et al., 2007. The amount of recycled crust in sources of mantle-derived melts. *Science* 316, 412–417.
- Spiegelman, M., Elliott, T., 1993. Consequences of melt transport for uranium series disequilibrium in young lavas. *Earth Planet. Sci. Lett.* 118, 1–20.
- Spiegelman, M., Kenyon, P.M., 1992. The requirement of chemical disequilibrium during magma migration. *Earth Planet. Sci. Lett.* 109, 611–620.
- Suetsugu, D., Inoue, T., Yamada, A., Zhao, D., Obayashi, M., 2006. Towards mapping three-dimensional distribution of water in the transition zone from P-wave velocity tomography and 660-km discontinuity depths. In: Jacobsen, S.D., Lee, S.v.d. (Eds.), *Earth's Deep Water Cycle*. American Geophysical Union, Washington DC, pp. 237–249.
- Takei, Y., 2002. Effect of pore geometry on Vp/Vs: from equilibrium geometry to crack. *J. Geophys. Res.* 107. doi:10.1029/2001JB000522.
- Tarits, P., Hautot, S., Perrier, F., 2004. Water in the mantle: results from electrical conductivity beneath the French Alps. *Geophys. Res. Lett.* 31. doi:10.1029/2003GL019277.
- Tauzin, B., Debayle, E., Wittingger, G., 2010. Seismic evidence for a global low-velocity layer within the Earth's upper mantle. *Nat. Geosci.* 3, 718–721.
- Toffelmier, D.A., Tyburczy, J.A., 2007. Electromagnetic detection of a 410-km-deep melt layer in the southwestern United States. *Nature* 447, 991–994.
- Tolstikhin, I.N., Hofmann, A.W., 2005. Early crust on top of the Earth's core. *Phys. Earth Planet. Inter.* 148, 109–130.
- Utada, H., Koyama, T., Obayashi, M., Fukao, Y., 2009. A joint interpretation of electromagnetic and seismic tomography models suggests the mantle transition zone below Europe is dry. *Earth Planet. Sci. Lett.* 281, 249–257.
- Utada, H., Koyama, T., Shimizu, H., Chave, A.D., 2003. A semi-global reference model for electrical conductivity in the mid-mantle beneath the north Pacific region. *Geophys. Res. Lett.* 30. doi:10.1029/2002GL016092.
- van der Meijde, M., Marone, F., Giardini, D., van der Lee, S., 2003. Seismic evidence for water deep in Earth's upper mantle. *Science* 300, 1556–1558.
- Wang, D., Mookherjee, M., Xu, Y., Karato, S., 2006. The effect of water on the electrical conductivity in olivine. *Nature* 443, 977–980.
- Wang, W., Takahashi, E., 2000. Subsolidus and melting experiments of K-doped peridotite KLB-1 to 27 GPa; its geophysical and geochemical implications. *J. Geophys. Res.* 105, 2855–2868.
- Weidner, D.J., Wang, Y., 2000. Phase transformations: implications for mantle structure. In: Karato, S., Forte, A.M., Liebermann, R.C., Masters, G., Stixrude, L. (Eds.), *Earth's Deep Interior: Mineral Physics and Tomography*. American Geophysical Union, Washington DC, pp. 215–235.
- Wood, B.J., 1995. The effect of H₂O on the 410-kilometer seismic discontinuity. *Science* 268, 74–76.
- Wood, B.J., Corgne, A., 2007. Mineralogy of the Earth—trace elements and hydrogen in the Earth's transition zone and lower mantle. In: Price, G.D. (Ed.), *Treatise on Geophysics*. : Mineral Physics, 2. Elsevier, Amsterdam, pp. 63–89.
- Xu, Y., Shankland, T.J., Duba, A.G., 2000. Pressure effect on electrical conductivity of mantle olivine. *Phys. Earth Planet. Inter.* 118, 149–161.
- Yoshino, T., 2010. Laboratory electrical conductivity measurement of mantle minerals. *Surv. Geophys.* 31, 163–206.
- Yoshino, T., Mantilake, G., Matsuzaki, T., Katsura, T., 2008a. Dry mantle transition zone inferred from the conductivity of wadsleyite and ringwoodite. *Nature* 451, 326–329.
- Yoshino, T., Matsuzaki, T., Shatskiy, A., Katsura, T., 2009. The effect of water on the electrical conductivity of olivine aggregates and its implications for the electrical structure of the upper mantle. *Earth Planet. Sci. Lett.* 288, 291–300.
- Yoshino, T., Matsuzaki, T., Yamashita, S., Katsura, T., 2006. Hydrous olivine unable to account for conductivity anomaly at the top of the asthenosphere. *Nature* 443, 974–976.
- Yoshino, T., Nishi, M., Matsuzaki, T., Yamazaki, D., Katsura, T., 2008b. Electrical conductivity of majorite garnet and its implications for electrical structure in the mantle transition zone. *Phys. Earth Planet. Inter.* 170, 193–200.
- Yoshino, T., Nishihara, Y., Karato, S., 2007. Complete wetting of olivine grain-boundaries by a hydrous melt near the mantle transition zone. *Earth Planet. Sci. Lett.* 256, 466–472.
- Zener, C., 1941. Theory of the elasticity of polycrystals with viscous grain boundaries. *Phys. Rev.* 60, 906–908.



Shun-ichiro Karato is a geophysicist who conducts interdisciplinary studies encompassing mineral physics and geodynamics. He combines studies on the properties of minerals at the atomic scale with global scale geophysical observations to understand the dynamics and evolution of Earth and planets. He earned BSc, MSc and PhD from University of Tokyo in 1972, 1974 and 1977 respectively and held faculty positions at University of Tokyo (1977–1989) and University of Minnesota (1989–2001) before moving to Yale University in 2001.

Supplemental Materials 1. Seismic wave velocities in mantle minerals

When anelastic relaxation occurs with the absorption band, then the functional relationship between seismic wave velocity and various parameters can be written as (Karato, 1995; Karato, 2008), viz.,

$$V_{S/P}(T, C_W, \omega, X) = V_{S/P}^{\infty}(T, C_W, X) \cdot \left[1 - \frac{\cot \frac{\alpha}{2}}{2} Q_{S/P}^{-1}(T, C_W, \omega, X) \right] \quad (\text{S1-1})$$

where $V_{S/P}(T, C_W, \omega, X)$ is the S- or P-wave velocity at seismic frequencies, T is temperature and C_W is water content and X is the major element chemistry (e.g., $Mg\#$). $V_{S/P}^{\infty}(T, C_W, X)$ are the S- or P-wave velocities at infinite frequency (velocity without the influence of anelasticity), and $Q_{S/P}^{-1}(T, C_W, X)$ is energy dissipation associated with wave propagation, and α is a parameter representing the frequency dependence, i.e., $Q^{-1} \propto \omega^{-\alpha}$ (a typical value is $\alpha \sim 0.3$ (Karato, 2008)). The high frequency, anharmonic term depends nearly linearly on temperature and water content, viz.,

$$V_{S/P}^{\infty}(T, C_W) \approx V_{S/P,0}^{\infty} \cdot \left(1 - \beta_{S/P,T}(T - T_0) - \beta_{S/P,W}(C_W - C_{W0}) \right) \quad (\text{S1-2})$$

where $\beta_{S/P,T}$ and $\beta_{S/P,W}$ are the parameters representing the temperature and water sensitivity of infinite frequency seismic wave velocities. Most of the experimental studies on seismic wave velocities are conducted at high frequencies (100 MHz or higher). Under

these conditions, the effects of anelasticity are small and only $V_{S/P}^{\infty}(T, C_W, X)$ can be investigated.

The water effect might be enhanced at lower frequencies through the influence of anelasticity (KARATO, 1995; KARATO, 2003). However, only very preliminary studies are available to test this model (AIZAWA et al., 2008; JACKSON et al., 1992). However, knowing that $\alpha \sim 0.3$, one can obtain a rough estimate of the magnitude of this effect from the observed seismic wave attenuation. For instance, $Q_s = 143$ in the MTZ for PREM, and therefore the anelasticity correction factor is $\sim 0.7\%$. Assuming that Q_s varies by a factor of ~ 2 by the variation in water content in the transition zone (GUNG and ROMANOWICZ, 2004), the corresponding variation in velocity is $\sim 0.4\%$, which is only marginally observable. We conclude that the influence of water on seismic wave velocities is small, less than $\sim 0.5\%$.

In contrast, there are experimental results that indicate that the influence of major element composition on seismic wave velocities is large, up to a few %. The most obvious heterogeneity in major element composition is the contrast between “depleted” and undepleted peridotite, namely harzburgite and pyrolite. Peridotites with these different compositions have different mineralogy mostly due to the difference in the abundance of majorite garnet (in most of the MTZ; (IRIFUNE et al., 2008)) and Ca-perovskite (in the lower part of the MTZ; (IRIFUNE and RINGWOOD, 1987)). This results in a large difference in seismic wave velocities. Using (IRIFUNE et al., 2008) data, I estimate that the difference between pyrolite and harzburgite results in a velocity difference of $\sim 3-4\%$ in the main portion of the MTZ. In the deep portion, the difference can be larger ($\sim 5\%$) due to the difference in the content of Ca-perovskite (NISHIYAMA et

al., 2009). Also minerals in depleted and undepleted materials have different $Mg\#$ that also affects seismic wave velocities.

Supplemental Materials 2. Electrical conductivity in mantle minerals

Influence of major element chemistry

The influence of $Mg\#$ ($100 \times \frac{Mg}{Mg+Fe}$) on electrical conductivity was studied for olivine (CEMIČ et al., 1980) and for garnet (ROMANO et al., 2006) for polaron conduction. In both cases, the increase in $Mg\#$ reduces electrical conductivity. This trend is consistent with the fact that the defect concentrations in these minerals decrease with $Mg\#$. There is no detailed studies on the influence of $Mg\#$ on proton conduction. However, using the results by (ZHAO et al., 2004) on the influence of $Mg\#$ on the solubility of hydrogen in olivine, one can make a reasonable estimate on the influence of $Mg\#$ on proton conduction. These results can be parameterized in terms of the dependence of the pre-exponential factor on $Mg\#$ viz.,

$$\frac{A}{A_0} = \exp(\varphi \cdot (Mg\#_0 - Mg\#)) \quad (S2-1)$$

where φ (~ 0.2) is a non-dimensional parameter (e.g., (ROMANO et al., 2006)). The variation in $Mg\#$ for ± 2 from a standard value of $Mg\#=90$ (WALTER, 2005) will change the electrical conductivity only by a factor of $\sim 50\%$.

The main consequence of the variation in Al and Ca is the variation in the fraction of garnet. However, the influence of the change in the volume fraction of garnet is not large (less than a factor of ~ 2) either due to the small volume fraction (in the upper mantle), or to the relatively low conductivity due to a smaller hydrogen content (in the MTZ).

Influence of oxygen fugacity

Influence of oxygen fugacity on electrical conductivity in olivine was studied for hopping conduction (SCHOCK and DUBA, 1985). A similar result was reported for wasdleyite for hopping (polaron) conduction (Dai and Karato, 2009b). The influence of oxygen fugacity for proton conduction is opposite (Dai and Karato, 2009b). This can be interpreted by a model of point defects in these minerals: the concentration of ferric iron (the charge carrier for polaron conduction) increases with oxygen fugacity, whereas the concentration of proton decreases with oxygen fugacity.

Influence of pressure

Influence of pressure on electrical conductivity is modest but is potentially important in the upper mantle where the pressure can change up to ~13 GPa. So let me focus on the possible role of pressure on electrical conductivity in the upper mantle minerals. The influence of pressure on hopping (polaron) conduction in olivine was studied by (XU et al., 2000). The influence of pressure on both proton and hopping conduction was studied for pyrope garnet by (Dai and Karato, 2009a). In all cases, the influence of pressure is relatively small: a change in pressure by $\Delta P = 5$ GPa results in the change in conductivity by less than a factor of ~3.

The recent results by (YOSHINO et al., 2009) on proton conduction in olivine at 10 GPa showed a factor of ~10 lower conductivity compared to the results by (WANG et al., 2006) measured at 4 GPa. Since both studies are on olivine polycrystals using the impedance spectroscopy, it is possible that the discrepancy between these two studies is due to the influence of pressure. Since causes for this difference is unknown, I used

models for olivine conductivity with this large pressure effect as well as without such an effect.

Water content dependence of activation energy

In general, the activation energy for some transport processes could depend on the composition of a material. Well known is the dependence of activation energy for diffusion or creep on $Mg\#$ that can be explained by the homologous temperature model (e.g., (Karato, 2008)). (Yoshino et al., 2008) argued that the activation energy for electrical conductivity for “wet” wadsleyite depends strongly on water content. However, (Karato and Dai, 2009) and (Karato and Dai, 2009) showed that a large part of the observations by (Yoshino et al., 2008) is caused by the artifact of using low-frequency measurements. In fact, a later study by (Yoshino et al., 2009) on hydrous olivine where they used the impedance spectroscopy, they did not find strong dependence of activation energy on water content. In fact, a model for the strong compositional dependence of activation energy proposed by (Pearson and Bardeen, 1949) assumes that all impurities have effective charge. According to the model by (Karato, 2006), a majority of hydrogen in mantle minerals has no effective charge (two protons trapped at M-site), and only a small fraction of mobile hydrogen contribute to electrical conductivity. In this model, the use of a model by (Pearson and Bardeen, 1949) is not appropriate, and in fact, the experimental observations do not support such a model. A large difference in activation energy between diffusion of hydrogen (~ 120 kJ/mol for wadsleyite; (Hae et al., 2006)) and electrical conductivity (~ 88 kJ/mol: (Dai and Karato, 2009b)) also supports a notion

that not all the hydrogen are involved in electrical conductivity as originally supposed by (Karato, 1990).

Conductivity of an aggregate

Given the mineralogy and element partitioning for each mineral, and temperature (pressure) and oxygen fugacity, one can calculate electrical conductivity of each mineral, and then using a model for a conductivity of an aggregate, one can calculate the aggregate conductivity. Several models have been proposed to calculate the aggregate conductivity (McLachlan et al., 1990), but here I use the Hashin-Shtrikman average. The upper bound by this method is given by

$$\sigma_{HS}^+ = \sigma_n + \frac{A^+}{1 - \frac{A^+}{3\sigma_n}} \quad (\text{S2-2})$$

with $A^+ = \sum_{i=1}^{n-1} \frac{f_i}{\frac{1}{(\sigma_i - \sigma_n)} + \frac{1}{3\sigma_n}}$ where f_i is the volume fraction of the i -th component, σ_i is

the conductivity of the i -th component, and σ_n is the maximum conductivity, and the lower bound is given by

$$\sigma_{HS}^- = \sigma_1 + \frac{A^-}{1 - \frac{A^-}{3\sigma_1}} \quad (\text{S2-3})$$

with $A^- = \sum_{i=2}^n \frac{f_i}{\frac{1}{(\sigma_i - \sigma_1)} + \frac{1}{3\sigma_1}}$ and σ_1 is the minimum conductivity (Hashin and Shtrikman,

1962). The upper (lower) bound provides a good estimate when volumetrically dominant

phase has the highest (lowest) conductivity. For “dry” upper mantle, volumetrically minor component, garnet, has the highest conductivity and hence the lower bound is a good approximation. However, in other cases, the volumetrically dominant mineral (olivine, wadsleyite or ringwoodite) has the highest conductivity, and the upper bound gives a good estimate. However, the difference between the upper and the lower bound is not large, less than ~50% in most cases.

Supplemental Materials 3. Evolution of the ocean mass

In a conventional model of water circulation, mantle is treated as a single unit (Franck and Bounama, 1995; Franck and Bounama, 2001; McGovern and Schubert, 1989; Rüpke et al., 2006). In such a model, the evolution of ocean mass and of mantle water content can be described by (Rüpke et al., 2006),

$$\frac{dX^{ocean}}{dt} = \frac{1}{\tau_1} X^{mantle} - R = \frac{1}{\tau_1} (X^{total} - X^{ocean}) - R \quad (S3-1)$$

and

$$\frac{dX^{mantle}}{dt} = -\frac{1}{\tau_1} X^{mantle} + R \quad (S3-2)$$

where X^{mantle} is the mantle water mass, X^{ocean} is the ocean water mass, τ_1 is the mantle degassing time constant, and R is the mantle regassing rate. It is assumed that the total water content of Earth, $X^{total} = X^{mantle} + X^{ocean}$, is constant.

Let us consider, for simplicity, a case where the water content is controlled by the *dynamic equilibrium*. In such a case,

$$\bar{X}^{ocean} = X^{total} - \tau_1 R \quad (S3-3)$$

and

$$\bar{X}^{mantle} = \tau_1 R. \quad (S3-4)$$

Note that in the single component mantle model described above, the ocean mass and water content in the mantle are highly sensitive to the variation in regassing rates in this model. Indeed (Franck and Bounama, 2001) showed such a high sensitivity of ocean mass (mantle water) to the change in regassing rate in their numerical modeling.

A quite different situation arises when the role of mid-mantle partial melting is considered. I consider a model where Earth is made of three regions, i.e., the oceans, the upper mantle, and the deep mantle. Between each region I assume exchange of water but the total water content is kept constant (**Figure S3-1**). Degassing occurs not only from the upper mantle at mid-ocean ridges, but also from the deep mantle (OIB source regions). In this model, there are two independent variables to describe the water content of the mantle, i.e., the water mass of the upper mantle, X^{UM} , and the water mass of the deep mantle, X^{DM} . Under these assumptions, the mass conservation considerations lead to the following relationships,

$$\frac{dX^{ocean}}{dt} = \frac{X^{UM}}{\tau_1} + \frac{X^{DM}}{\tau_2} - R \quad (S3-5)$$

$$\frac{dX^{UM}}{dt} = -\frac{X^{UM}}{\tau_1} + \beta R + Y \quad (S3-6)$$

and

$$\frac{dX^{DM}}{dt} = -\frac{X^{DM}}{\tau_2} + (1 - \beta)R - Y \quad (S3-7)$$

where $\tau_{1,2}$ is the characteristic time of degassing from the upper mantle and from the deep mantle respectively, Y represents the water transport rate between the deep mantle and the upper mantle at 410-km discontinuity (I used the fact that the net internal water

transport between the upper mantle and the deep mantle is zero), β is the fraction of water transported to the upper mantle by subduction and R is the total rate of water input to the mantle (regassing rate) by subduction.

The details of this internal water transport depend on the processes in the mantle such as partial melting at ~410-km depth (Karato et al., 2006; Leahy and Bercovici, 2007; Richard et al., 2006). However, without going to the details, one can obtain some important general conclusions. First, because of the presence of another degree of freedom, the upper mantle water mass ($X^{UM} (= M^{UM} x^{UM})$), M^{UM} : mass of the upper mantle) and the deep mantle water mass ($X^{DM} (= M^{DM} x^{DM})$), M^{DM} : mass of the deep mantle) are generally different in this model (therefore water content, $x^{UM, DM}$, will also be different), which is consistent with the inferred layered water content in the mantle. Physically, this corresponds to the presence of some processes such as mid-mantle partial melting.

Second, because of the presence of two different water reservoirs, the ocean mass is only indirectly connected to the regassing rate, and the sensitivity of the ocean mass to degassing/regassing rate can be reduced. This can be understood by considering a limiting case where we have a dynamic equilibrium. The rate of water transfer, Y , from the MTZ to the upper mantle is controlled by the nature of partial melting at 410-km. In the model by (Bercovici and Karato, 2003), fractional melting and the dense melt is assumed. Therefore the water flux there is proportional to the fraction of solid that goes to the upper mantle (and the water content of the solid). From the “lever rule”, this fraction is $(x^l - x)/(x^l - x^s)$ (x^l : water concentration at the liquidus, x^s : water

concentration at the liquidus, x : water content in the MTZ (DM)). Consequently one obtains, $Y = \frac{1}{\tau_3} (X^l - X^{DM})$ where $X^l = M^{DM} x^l$ (τ_3 : characteristic time for the water transport from the deep mantle to the upper mantle). The steady-state ocean mass corresponding to this model is given by

$$\bar{X}^{ocean} = X^{total} - \xi \tau_1 R - \zeta X^l \quad (S3-8)$$

with $\xi = 1 - \frac{\tau_3}{\tau_1} \frac{\tau_2 - \tau_1}{\tau_2 - \tau_3} (1 - \beta)$ and $\zeta = \frac{\tau_2 - \tau_1}{\tau_2 - \tau_3}$. If $\xi < 1$ then the ocean mass is less sensitive to the fluctuation in regassing rate than for the single-stage model. Such a condition is met if $\frac{\tau_2 - \tau_1}{\tau_2 - \tau_3} > 0$. Because of the smaller volume flux of plumes than the upwelling flux at mid-ocean ridges (Labrosse, 2002; Sleep, 1990), it is likely that $\tau_2 - \tau_1 > 0$. So this condition will be met if $\tau_2 - \tau_3 > 0$. Not much is known about τ_3 , but since τ_2 is expected to be much larger than τ_1 (~ 1 Gyrs, (McGovern and Schubert, 1989)), it is plausible that $\tau_2 - \tau_3 > 0$ ((Leahy and Bercovici, 2010) presented a model suggesting a relatively short time-scale of mass exchange, 0.3-0.5 Gyrs, between the MTZ and the upper mantle). Note also that the ocean mass is more stable when $(1 - \beta)$ is larger, i.e., when more water goes to the deep mantle. Obviously, the above model over-simplifies water cycling processes, and one needs a more complete analysis including time-dependent behavior to understand the evolution of the ocean mass through the global water cycle.

References

- Aizawa, Y. et al., 2008. Seismic properties of Anita Bay dunite: An exploratory study of the influence of water. *Journal of Petrology*, 49: 841-855.
- Bercovici, D. and Karato, S., 2003. Whole mantle convection and transition-zone water filter. *Nature*, 425: 39-44.
- Cemič, L., Will, G. and Hinze, E., 1980. Electrical conductivity measurements on olivines Mg_2SiO_4 - Fe_2SiO_4 under defined thermodynamic conditions. *Physics and Chemistry of Minerals*, 6: 95-107.
- Dai, L. and Karato, S., 2009a. Electrical conductivity of pyrope-rich garnet at high temperature and pressure. *Physics of the Earth and Planetary Interiors*, 176: 83-88.
- Dai, L. and Karato, S., 2009b. Electrical conductivity of wadsleyite under high pressures and temperatures. *Earth and Planetary Science Letters*, 287: 277-283.
- Franck, S. and Bounama, C., 1995. Effects of water-dependent creep rate on the volatile exchange between mantle and surface reservoirs. *Physics of Earth and Planetary Interiors*, 92: 57-65.
- Franck, S. and Bounama, C., 2001. Global water cycle and Earth's thermal evolution. *Journal of Geodynamics*, 32: 231-246.
- Gung, Y. and Romanowicz, B., 2004. Q tomography of the upper mantle using three-component long-period waveforms. *Geophysical Journal International*, 157: 813-830.

- Hae, R., Ohtani, E., Kubo, T., Koyama, T. and Utada, H., 2006. Hydrogen diffusivity in wadsleyite and water distribution in the mantle transition zone. *Earth and Planetary Science Letters*, 243: 141-148.
- Hashin, Z. and Shtrikman, S., 1962. A variational approach to the theory of effective magnetic permeability of multiphase materials. *Journal of Applied Physics*, 33: 3125-3131.
- Irifune, T., Higo, Y., Inoue, T., Ohfuji, H. and Funakoshi, K., 2008. Sound velocities of majorite garnet and the composition of the mantle transition zone. *Nature*, 451: 814-817.
- Irifune, T. and Ringwood, A.E., 1987. Phase transformations in primitive MORB and pyrolyte composition to 25 GPa and some geophysical implications. In: M.H. Manghnani and Y. Syono (Editors), *High-Pressure Research in Mineral Physics*. American Geophysical Union, Washington DC, pp. 231-242.
- Jackson, I., Paterson, M.S. and Fitz Gerald, J.D., 1992. Seismic wave dispersion and attenuation in Åheim dunite. *Geophysical Journal International*, 108: 517-534.
- Karato, S., 1990. The role of hydrogen in the electrical conductivity of the upper mantle. *Nature*, 347: 272-273.
- Karato, S., 1995. Effects of water on seismic wave velocities in the upper mantle. *Proceedings of the Japan Academy*, 71: 61-66.
- Karato, S., 2003. Mapping water content in Earth's upper mantle. In: J.E. Eiler (Editor), *Inside the Subduction Factory*. American Geophysical Union, Washington DC, pp. 135-152.

- Karato, S., 2006. Influence of hydrogen-related defects on the electrical conductivity and plastic deformation of mantle minerals: A critical review. In: S.D. Jacobsen and S. van der Lee (Editors), *Earth's Deep Water Cycle*. American Geophysical Union, Washington DC, pp. 113-129.
- Karato, S., 2008. *Deformation of Earth Materials: Introduction to the Rheology of the Solid Earth*. Cambridge University Press, Cambridge, 463 pp.
- Karato, S., Bercovici, D., Leahy, G., Richard, G. and Jing, Z., 2006. Transition zone water filter model for global material circulation: Where do we stand? In: S.D. Jacobsen and S. van der Lee (Editors), *Earth's Deep Water Cycle*. American Geophysical Union, Washington DC, pp. 289-313.
- Karato, S. and Dai, L., 2009. Comments on "Electrical conductivity of wadsleyite as a function of temperature and water content" by Manthilake et al. *Physics of the Earth and Planetary Interiors*, 174: 19-21.
- Labrosse, S., 2002. Hotspots, mantle plumes and core heat loss. *Earth and Planetary Science Letters*, 199: 147-156.
- Leahy, G. and Bercovici, D., 2007. On the dynamics of hydrous melt layer above the transition zone. *Journal of Geophysical Research*, 112: 10.1029/2006JB004631.
- Leahy, G.M. and Bercovici, D., 2010. Reactive infiltration of hydrous melt above the mantle transition zone. *Journal of Geophysical Research*, 115: 10.1029/2009JB006757.
- McGovern, P.J. and Schubert, G., 1989. Thermal evolution of the Earth: effects of volatile exchange between atmosphere and interior. *Earth and Planetary Science Letters*, 96: 27-37.

- McLachlan, D.S., Blazskiewicz, M. and Newnham, R.E., 1990. Electrical resistivity of composite. *Journal of the American Ceramic Society*, 73: 2187-2203.
- Nishiyama, N., Kato, T., Irifune, T. and Wada, K., 2009. Phase relations in harzburgite: Stagnation of harzburgite at the lower part of the mantle transition zone and interpretation of seismic discontinuity at 600 km depth. *EOS*: in press.
- Pearson, G.L. and Bardeen, J., 1949. Electrical conductivity of pure silicon and silicon alloys containing boron and phosphorus. *Physical Review*, 75: 865-883.
- Richard, G., Bercovici, D. and Karato, S., 2006. Slab dehydration in the Earth's mantle transition zone. *Earth and Planetary Science Letters*, 251: 156-167.
- Romano, C., Poe, B.T., Kredie, N. and McCammon, C., 2006. Electrical conductivity of pyrope-almandine garnets up to 19 GPa and 1700°C. *American Mineralogist*, 91: 1371-1377.
- Rüpke, L.H., Phipps Morgan, J. and Dixon, J.E., 2006. Implications of subduction rehydration for Earth's deep water cycle. In: S.D. Jacobsen and S.v.d. Lee (Editors), *Earth's Deep Water Cycle*. American Geophysical Union, Washington DC, pp. 263-276.
- Schock, R.N. and Duba, A., 1985. Point defects and the mechanisms of electrical conduction in olivine. In: R.N. Schock (Editor), *Point Defects in Minerals*. American Geophysical Union, Washington DC, pp. 88-96.
- Sleep, N.H., 1990. Hotspots and mantle plumes: some phenomenology. *Journal of Geophysical Research*, 95: 6715-6736.

- Walter, M.J., 2005. Melt extraction and compositional variability in mantle lithosphere. In: R.W. Carlson (Editor), *Treatise on Geochemistry* Elsevier, Amsterdam, pp. 363-394.
- Wang, D., Mookherjee, M., Xu, Y. and Karato, S., 2006. The effect of water on the electrical conductivity in olivine. *Nature*, 443: 977-980.
- Xu, Y., Shankland, T.J. and Duba, A.G., 2000. Pressure effect on electrical conductivity of mantle olivine. *Physics of the Earth and Planetary Interior*, 118: 149-161.
- Yoshino, T., Manthilake, G., Matsuzaki, T. and Katsura, T., 2008. Dry mantle transition zone inferred from the conductivity of wadsleyite and ringwoodite. *Nature*, 451: 326-329.
- Yoshino, T., Matsuzaki, T., Shatskiy, A. and Katsura, T., 2009. The effect of water on the electrical conductivity of olivine aggregates and its implications for the electrical structure of the upper mantle. *Earth and Planetary Science Letters*, 288: 291-300.
- Zhao, Y.-H., Ginsberg, S.B. and Kohlstedt, D.L., 2004. Solubility of hydrogen in olivine: dependence on temperature and iron content. *Contributions to Mineralogy and Petrology*, 147: 155-161.

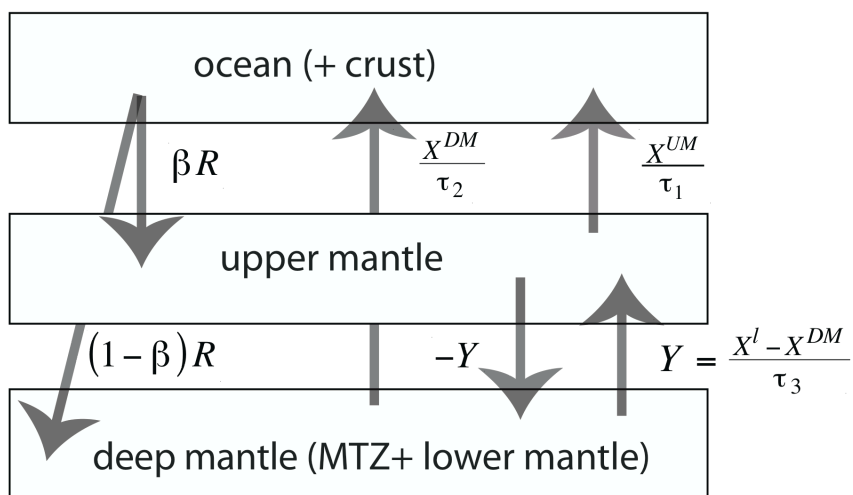


Fig. S3-1